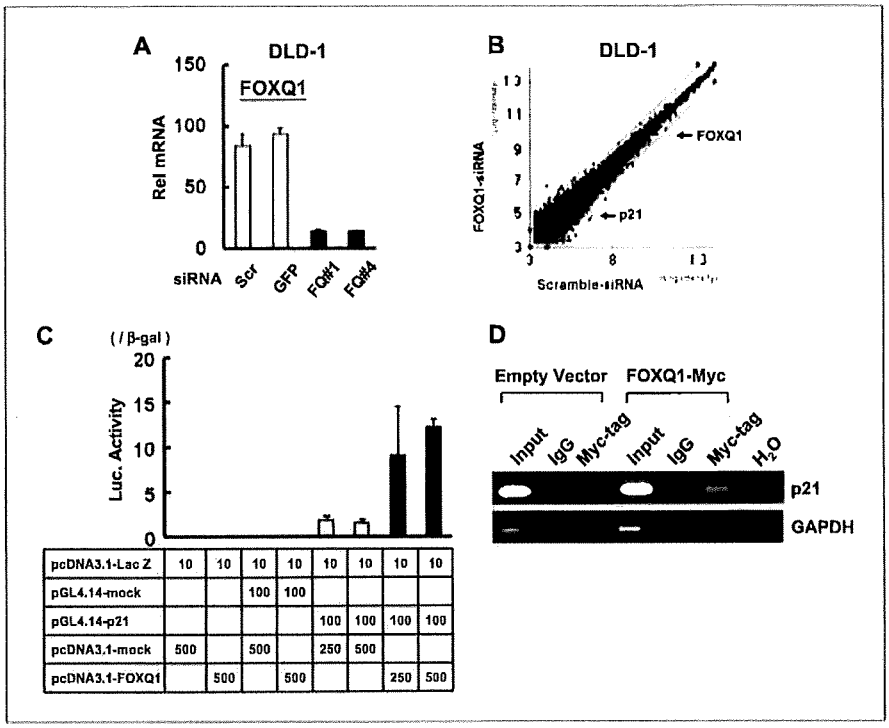

pcDNA3.1-Lac Z	10	10	10	10	10	10	10	10
pGL4.14-mock			100	100				
pGL4.14-p21					100	100	100	100
pcDNA3.1-mock	500		500		250	500		
pcDNA3.1-FOXQ1		500		500			250	500

Figure 2. FOXQ directly regulates *p21* transcription. A, FOXQ1-targeting siRNA (FQ#1 and FQ#4) suppressed FOXQ1 expression in DLD-1 cells. The mRNA expression levels of *FOXQ1* were determined using real-time RT-PCR. B, microarray analysis of DLD-1 cells transfected with control-siRNA or FOXQ1-siRNA. The longitudinal axis indicates the mRNA expression of FOXQ1-siRNA transfected cells and the horizontal axis indicates that of control-siRNA. Arrow, FOXQ1 or p21 expression. Each point indicates the normalized and log base 2 transformed microarray data. C, induction of p21 promoter activity by FOXQ1. Luciferase vectors with either an empty or p21 promoter (pGL4.14-mock or pGL4.14-p21) were transiently cotransfected with a mock or FOXQ1 expression plasmid (pcDNA3.1-mock or pcDNA3.1-FOXQ1) expressing β-galactosidase as an internal control. The results were normalized to β-galactosidase activity and are representative of at least three independent experiments. D, ChIP of FOXQ1 on the promoter of *p21*. HEK293 cells were transfected with empty vector (Myc) or Myc-tagged FOXQ1 vector. Agarose gel shows PCR amplification (35 cycles) of the *p21* promoter using inputs (1% of chromatin used for ChIP) or ChIPs as templates. Primers to the *GAPDH* promoter were used as the negative control.

Microarray analysis. The microarray procedure and analysis were performed according to the Affymetrix protocols and BRB Array Tools software, Ver. 3.3.0,[4] developed by Dr. Richard Simon and Dr. Amy Peng, as reported previously (21, 26).

Statistical analysis. The statistical analyses were performed using Microsoft Excel (Microsoft) to calculate the SD and to test for statistically significant differences between the samples using a Student's *t* test. A *P* value of <0.05 was considered statistically significant.

Results

FOXQ1 mRNA was overexpressed in CRCs. A microarray analysis for 10 paired CRC samples identified 30 genes as being significantly upregulated by >10-fold in CRC ($P < 0.001$; Supplementary Table S1). *FOXQ1*, an uncharacterized transcription factor, was upregulated by 28-fold in the CRC specimens (Fig. 1A), exhibiting the fourth highest level of upregulation [after interleukin-8, matrix metalloproteinase-1 (MMP), and MMP-3]. Real-time RT-PCR for the 10 paired samples and an additional 36 CRC samples showed that *FOXQ1* mRNA was markedly overexpressed in the CRC samples but was only expressed at a very low level in noncancerous colonic mucosa ($P < 0.001$; Fig. 1B). The average levels of *FOXQ1* expression were 299 ± 326 and 4.0 ± 5.0 ($\times 10^4$/GAPD), respectively.

FOXQ1 expression in normal tissues and cancer cell lines. To investigate the expression of *FOXQ1*, we analyzed the mRNA expression levels of *FOXQ1* in panels of human normal tissues and cancer cell lines using real-time RT-PCR. High levels of *FOXQ1* expression were observed in the stomach, salivary gland, prostate, trachea, and fetal liver among the 24 normal tissues that were examined (Fig. 1C, left). Relatively weak expression levels were detected in brain-derived tissues, kidney, lung, placenta, and thyroid gland. These results were consistent with those of a previous report (27).

[4] http://linus.nci.nih.gov/BRB-ArrayTools.html

In the cancer cell line panel, the mRNA expression levels of *FOXQ1* were higher in gastric cancer, CRC, and lung cancer cell lines than in the other cancer cell lines, indicating that the expression of *FOXQ1* varies among specific cancers (Fig. 1C, right). Interestingly, the overexpression of *FOXQ1* in CRC arose from normal colonic mucosa with very low expression levels during carcinogenesis.

p21 is a target gene of FOXQ1. To examine the function of FOXQ1 as a transcription factor and to explore its target genes, we performed a microarray analysis using a CRC cell line, DLD-1, transfected with FOXQ1-targeting siRNA or control siRNA. Two sequences of FOXQ1-siRNA, FQ#1 and FQ#4, were used to exclude the off-target effect of siRNA. Real-time RT-PCR showed that both sequences of FOXQ1-siRNA suppressed *FOXQ1* mRNA expression by ~80% in DLD-1 cells (Fig. 2A); thus, FQ#4 was used as the FOXQ1-siRNA in the following experiments. A microarray analysis showed that 19 genes were downregulated by FOXQ1-siRNA (Fig. 2B; Supplementary Table S2); *p21* was the fifth most-downregulated gene. Because p21 is a key regulator of cell cycle and apoptosis, we focused on p21 as a target molecule of FOXQ1.

To confirm the microarray data, p21 downregulation by FOXQ1-siRNA was examined using real-time RT-PCR and a

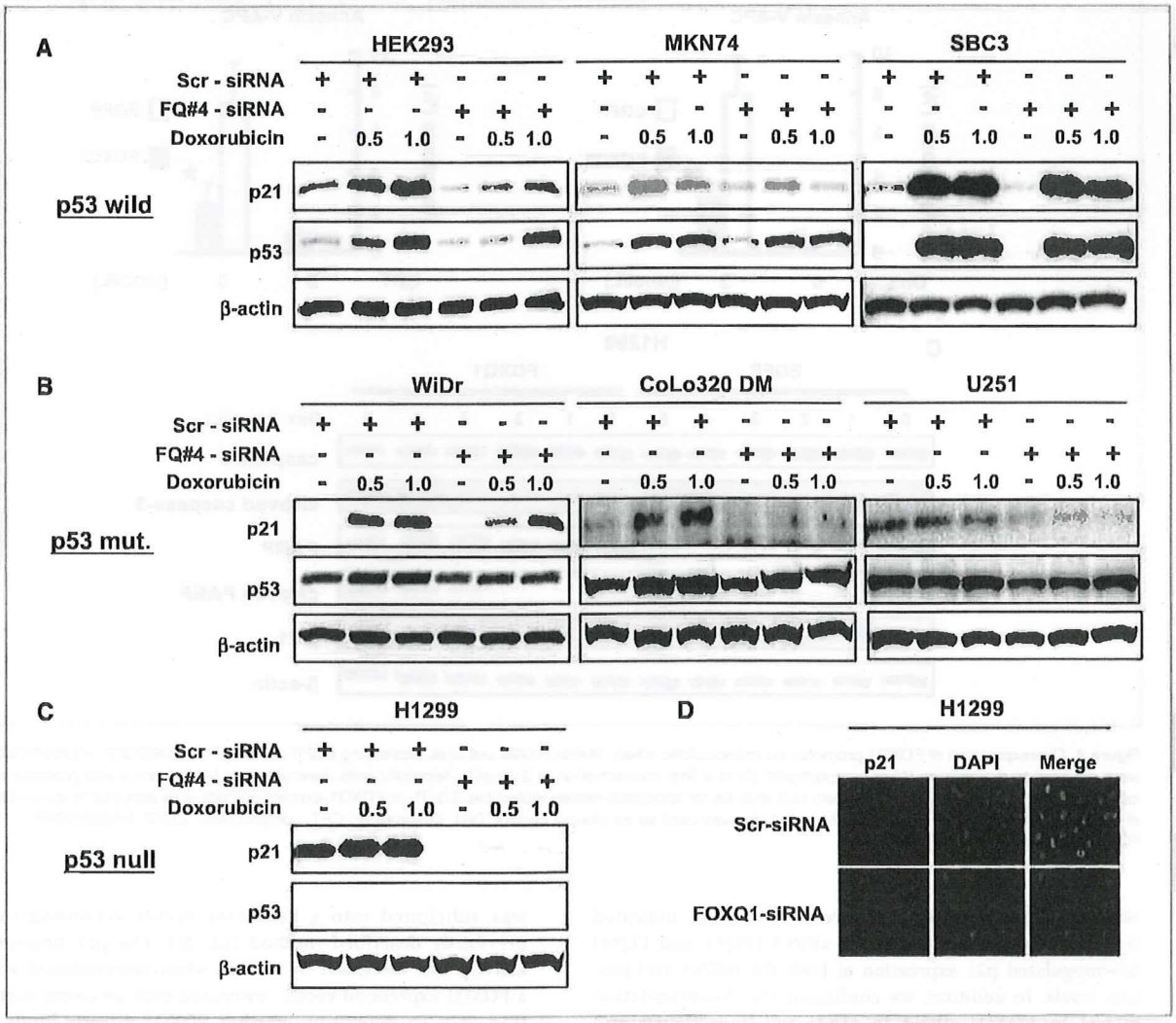

Figure 3. p21 induction by FOXQ1 and p53 status in cancer cells. The seven cell lines were transfected with control-siRNA or FOXQ1-siRNA for 24 h, and the cells were exposed to doxorubicin at a final concentration of 0.5 or 1 μmol/L for a further 24 h to enhance p21 induction. Western blot analyses for p21 and p53 were performed in three p53–wild type cell lines (A), three p53-mutant cell lines (B), and one p53-null cell line (C). The experiment was performed in duplicate. D, immunofluorescence p21 staining and 4′,6-diamidino-2-phenylindole (DAPI) staining for H1299 cells transfected with control-siRNA (top) or FOXQ1-siRNA (bottom) for 48 h. Scr, scramble-siRNA (control); FQ#4, FOXQ1-targeting siRNA. β-Actin was used as an internal control.

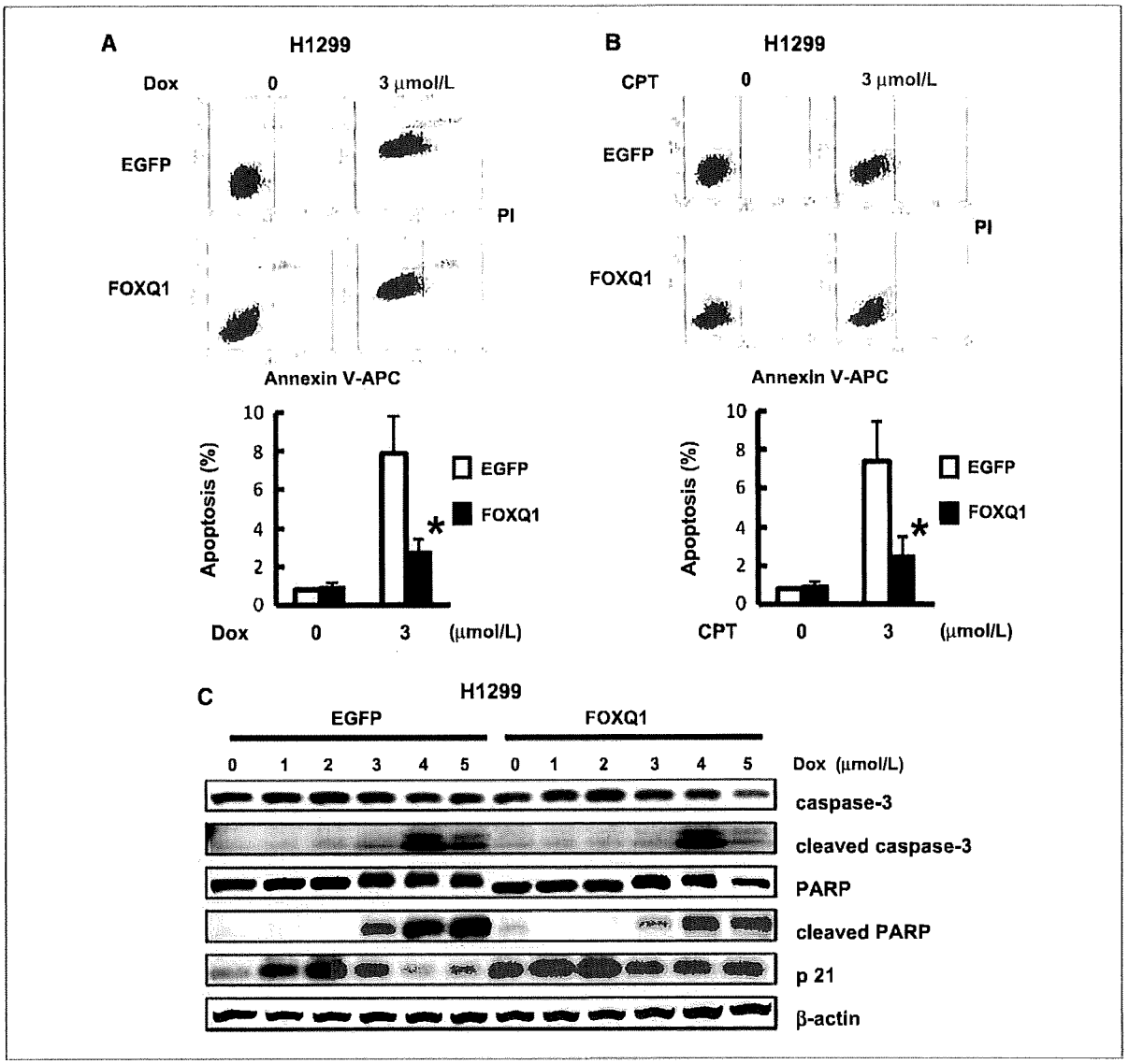

Figure 4. Overexpression of FOXQ1 promotes an antiapoptotic effect. Stable H1299 cell lines expressing EGFP or FOXQ1 (H1299/EGFP, H1299/FOXQ1) were exposed to doxorubicin (A) or camptothecin (B) at a final concentration of 3 μmol/L. Apoptotic cells were detected by Annexin V and propidium iodide (PI) using flow cytometry. C, Western blot analysis for apoptosis-related molecules. EGFP- or FOXQ1-expressing cells were exposed to doxorubicin at the indicated doses (0–5 μmol/L) for 24 h. β-Actin was used as an internal control. Dox, doxorubicin; CPT, camptothecin; EGFP, H1299/EGFP; FOXQ1, H1299/FOXQ1. *, $P < 0.05$.

Western blot analysis in DLD-1 cells. The results indicated that both sequences of FOXQ1-siRNA (FQ#1 and FQ#4) downregulated p21 expression at both the mRNA and protein levels. In addition, we confirmed the downregulation of p21 by FOXQ1-siRNA in other cell lines (WiDr and HEK293), obtaining similar results (Supplementary Fig. S1).

FOXQ1 directly increases the transcription activity of p21. We performed a luciferase reporter assay to determine whether FOXQ1 regulates p21 expression at the transcriptional level. A 2.4-kb section of the p21 promoter region was subcloned into a luciferase vector according to a previously described method (13, 28). The p21 promoter activity was increased by >8-fold when cotransfected with a FOXQ1 expression vector, compared with an empty vector (Fig. 2C). To determine whether FOXQ1 directly binds to p21 promoter, we transfected Myc or Myc-tagged FOXQ1 vectors into HEK293 cells and then conducted ChIP experiments. A segment of the *p21* promoter containing putative FOXQ1 binding site (−2264 to −1971) is precipitated with specific antibody, only if, FOXQ1 was induced (Fig. 2D).

The result indicates that FOXQ1 binds to the *p21* promoter and upregulates p21 transcriptional activity.

p53-independent p21 induction by FOXQ1 in cancer cells. Because p53 is the most important regulatory molecule of p21, we examined the downregulation of p21 by FOXQ1-siRNA in several cell lines with p53-wild type, p53-mutant, or p53-null statuses. These cell lines were transfected with control-siRNA or FOXQ1-siRNA, and p21 induction was enhanced by doxorubicin (29–31). The experiments were performed using three p53-wild type cell lines, three p53-mutation cell lines, and one p53-null cell line (Fig. 3A–C). Without doxorubicin exposure, all seven cell lines showed that p21 expression was downregulated by FOXQ1-siRNA. Notably, with doxorubicin exposure, considerable p21 downregulation by FOXQ1-siRNA was observed in the p53-mutation and p53-null cell lines, compared with in the p53-wild type cell lines. In the p53-null H1299 cell line, FOXQ1-siRNA completely suppressed p21 expression. These results suggest that p21 induction by FOXQ1 is p53 independent. An immunofluorescence study of p21 in H1299 cells also showed that p21 was completely downregulated by FOXQ1-siRNA (Fig. 3D).

Overexpression of FOXQ1 increases p21 expression and exhibits an antiapoptotic effect in cancer cells. Next, we established a stable *FOXQ1*-overexpressing cell line to confirm the induction of p21 expression by FOXQ1 and to detect any changes in the cellular phenotype of the cancer cells. FOXQ1 overexpression induced p21 expression (both mRNA and protein) in HEK293 and CoLo320 cells (Supplementary Fig. S1). Notably, p21 protein expression was markedly induced by >10-fold in the H1299/FOXQ1 cells (Supplementary Fig. S1). These results indicated that FOXQ1 robustly induces p21 expression, consistent with the findings of the siRNA study.

p21 induces an antiapoptotic effect and exerts a protective role against apoptosis induced by DNA damage. To

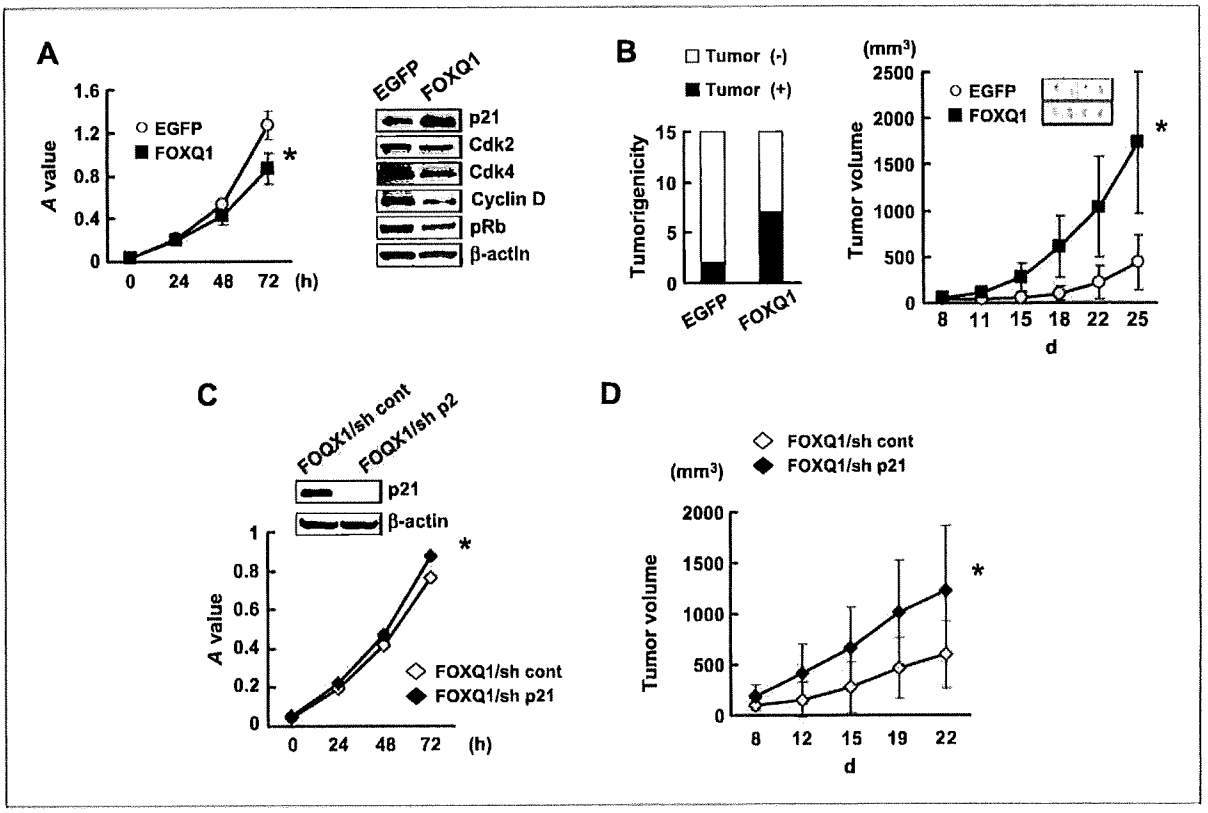

Figure 5. Overexpression of FOXQ1 enhances tumorigenicity and tumor growth *in vivo*. A, cellular growth and immunoblotting analysis of H1299 cell lines stably expressing EGFP or FOXQ1 (H1299/EGFP, H1299/FOXQ1). A total of 2×10^3 cells of each cell line were seeded in 96-well plates and evaluated after 0, 24, 48, and 72 h using MTT assay. Error bars, SD. Protein levels of H1299/EGFP and H1299/FOXQ1 cells were examined by Western blotting using specific antibody to p21, Cdk2, Cdk4, cyclin D, and phosphorylated Rb (pRb) protein. β-Actin was used as an internal control. EGFP, stable EGFP-overexpressing cells; FOXQ1, stable FOXQ1-overexpressing cells. B, H1299/EGFP and H1299/FOXQ1 cells were evaluated for their tumorigenicity *in vivo*. Mice ($n = 15$) were s.c. inoculated with a total of 1×10^6 cells. The numerical data indicate the number of mice. A total of 6×10^6 H1299/EGFP or H1299/FOXQ1 cells were s.c. inoculated into the right flank of each mouse to evaluate the tumor growth *in vivo* ($n = 12$). Representative H&E staining of tumor specimens was also shown. C, stable p21 knockdown or control cells obtained from H1299/FOXQ1 cells (H1299/FOXQ1/sh-control and H1299/FOXQ1/sh-p21) were evaluated for cellular growth and immunoblotting analysis. D, a total of 6×10^6 H1299/FOXQ1/sh-control or H1299/FOXQ1/sh-p21 cells were s.c. inoculated into the right flank of each mouse to evaluate the tumor growth ($n = 10$). *, $P < 0.05$.

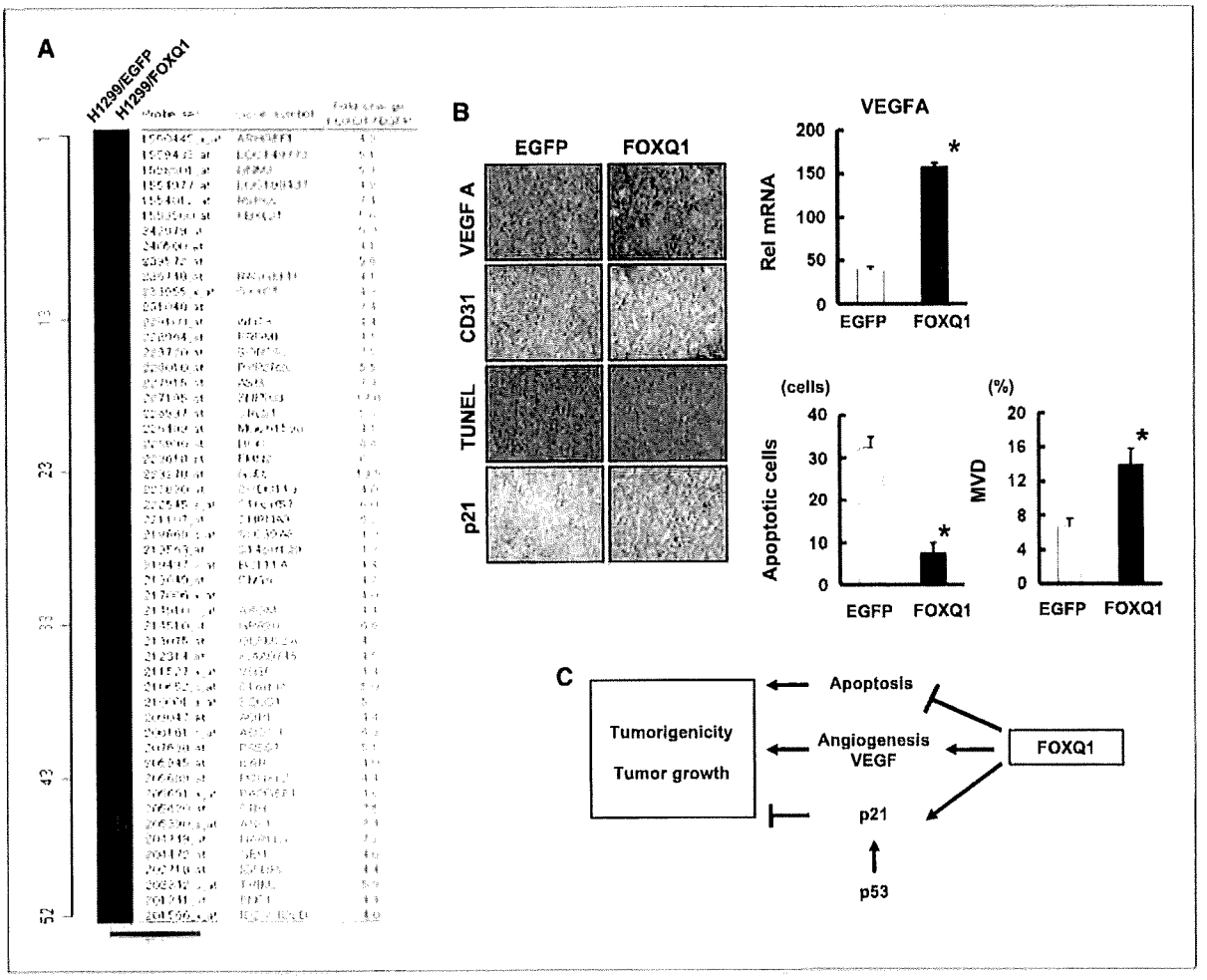

Figure 6. FOXQ1 promotes angiogenic and antiapoptotic effects *in vivo*. A, microarray analysis for H1299/EGFP or H1299/FOXQ1 cells. The upregulated genes over 4-fold by FOXQ1 were shown in the list. B, the mRNA expression levels of *VEGFA* were determined using a real-time RT-PCR analysis. Rel mRNA, normalized mRNA expression levels (*VEGFA/GAPD* x 10^4). VEGF, CD31, TUNEL, and p21 staining of tumor specimens inoculated with H1299/EGFP or H1299/FOXQ1 cells. Microvessel density (MVD) was determined by CD31-positive endothelial cells in tumor specimens using computer-assisted image analysis (Image J software package). C, diagram of a proposed mechanism of FOXQ1 for tumorigenicity and tumor growth. *, $P < 0.05$.

elucidate the role of apoptosis induced by FOXQ1 in cancer cells, we examined the apoptotic effect in H1299/EGFP and H1299/FOXQ1 cells using anticancer drugs. The overexpression of FOXQ1 inhibited the apoptosis induced by doxorubicin (H1299/EGFP: 7.9 ± 1.9%, H1299/FOXQ1: 2.7 ± 0.7%; Fig. 4A). Similarly, camptothecin-induced apoptosis was also inhibited in FOXQ1-overexpressing cells (H1299/EGFP: 7.4 ± 2.1%, H1299/FOXQ1: 2.5 ± 1.0%; Fig. 4B). Western blotting revealed that FOXQ1 overexpression decreased the levels of cleaved caspase-3 and cleaved PARP induced by doxorubicin (Fig. 4C). These results are consistent with those obtained using flow cytometry.

Overexpression of FOXQ1 decreases cellular proliferation but enhances tumorigenicity and tumor growth in vivo. Stable H1299/FOXQ1 cells showed decreased cellular proliferation compared with control cells *in vitro* (Fig. 5A). Expressions of Cdk4, cyclin D1, and Cdk2 were decreased by FOXQ1 expression in H1299/FOXQ1 cells and resulted in a decrease of phosphorylated Rb expression (Fig. 5A). To examine the biological functions of FOXQ1 overexpression *in vivo*, we evaluated tumorigenicity and tumor growth using H1299/EGFP or H1299/FOXQ1 cells. H1299/FOXQ1 cells exhibited a significantly elevated level of tumorigenesis *in vivo* (GFP 2/15, FOXQ1 7/15, $P < 0.05$; Fig. 5B). In addition, the tumor volume was markedly larger in H1299/FOXQ1 cells than in H1299/EGFP cells (EGFP: 437 ± 301, FOXQ1: 1735 ± 769 mm^3, $P < 0.001$; Fig. 5B) on day 25.

p21 does not contribute to FOXQ1-mediated tumor growth in vivo. Because emerging evidence has indicated that p21 may have dual functions with regard to tumor

progression and the suppression of cancer cells (32, 33), the shRNA targeting p21 or shRNA control viral vectors were further introduced into the H1299/FOXQ1 cells to elucidate the involvement of p21 in increased FOXQ1-mediated tumorigenicity and tumor growth *in vivo*. Stable H1299/FOXQ1/sh-p21 cells were slightly increased in cellular proliferation *in vitro* (Fig. 5C). In addition, tumor growth of H1299/FOXQ1/sh-p21 cells was increased compared with control cells *in vivo* (Fig. 5D). The results clearly indicate that p21 has negative roles for cellular proliferation and tumor growth in FOXQ1-overexpressing cells, suggesting that p21 does not contribute to FOXQ1-mediated tumor growth in FOXQ1-overexpressing cells *in vivo*.

***Overexpression of FOXQ1 promotes angiogenesis and antiapoptosis* in vivo.** To gain an insight into the mechanism by which FOXQ1 enhances tumor growth *in vivo*, we performed the microarray analysis on H1299/EGFP and H1299/FOXQ1 cells. Fifty-two genes were upregulated over 4-fold by overexpression of FOXQ1 including several genes that have positive roles for tumor growth, such as *VEGFA*, *WNT3A*, *RSPO2*, and *BCL11A* (Fig. 6A). Overexpression of FOXQ1 upregulated the *VEGFA* expression for 4.4-fold, suggesting the possibility of enhanced angiogenesis. Real-time RT-PCR for these cells and vascular endothelial growth factor (VEGF) staining of tumor specimens confirmed the result (Fig. 6B). Furthermore, CD31 staining of the tumor specimens showed that FOXQ1 overexpression significantly increased the angiogenesis *in vivo*.

Terminal deoxynucleotidyl transferase-mediated dUTP nick end labeling (TUNEL) and p21 immunostaining of the tumor specimens showed that p21 expression was increased and apoptosis was inhibited in H1299/FOXQ1 cells (Fig. 6B). These results strongly suggest that FOXQ1 promotes tumorigenicity and tumor growth with its angiogenic and antiapoptotic properties *in vivo* (Fig. 6C).

Discussion

FOX transcription factors are an evolutionarily conserved superfamily that control a wide spectrum of biological processes. Several Fox gene family members are involved in the etiology of cancer. Only the FOXO family has been regarded as *bona fide* tumor suppressors that promote apoptosis and cell cycle arrest at G_1 (34, 35). The loss of FOXO function observed in alveolar rhabdomyosarcoma through chromosomal translocation was first identified in relation to cancer. Many target genes of FOXO have been reported to date, including p21, cyclin D, Bim, TRAIL, and ER-α (36). On the other hand, the overexpression of FOXM is observed in head and neck cancer, breast cancer, and cervical cancer, and it enhances proliferation and tumor growth *in vitro* (37), suggesting that *FOXM* may be an oncogene. Although the available evidence is not conclusive, FOXP, FOXC, and FOXA have been linked to tumorigenesis and progression of certain cancers (36). Thus, the FOX family is thought to act as either an oncogene or a tumor suppressor. In the present study, we showed that the overexpression of FOXQ1 played a tumor-promoting role in CRC.

The p21 promoter region contains several definitive DNA regulatory elements, such as the p53-binding domain, E-box, Smad binding element, and TGF-β response elements. In the case of the other FOX family member FOXO, a recent report showed that the p21 promoter contains a consensus forkhead binding element (GGATCC) immediately upstream of the first Smad binding element and that the FOXO and Smad complexes activate p21 expression, whereas the FOXG1 protein binds to FOXO and blocks p21 induction (38). On the other hand, the consensus binding sequence (5′-NA(A/T)TGTTTA(G/T)(A/T)T-3′) has been defined for human FOXQ1 (4). The p21 promoter region contains several putative FOXQ1 binding sites according to its consensus binding sequence. Indeed, we have shown that FOXQ1 binds to a segment of the p21 promoter, indicating that FOXQ1 directly transactivates the p21 gene expression.

The initial descriptions of p21 were thought to indicate a tumor suppressor–like role, and p21 was almost solely regarded as a modulator with the principal function of inhibiting a cyclin-dependent kinase activity and, hence, cell cycle progression, because it was originally identified as a mediator of p53-induced growth arrest. However, emerging evidence has indicated that p21 may have dual functions with regard to tumor progression and the suppression of cancer cells, with examples of other genes with dual functions including TGF-β, Notch, Runx3, E2F, and p21 (32). Besides its growth inhibitory role, p21 is known to have a positive effect on cell proliferation (39–41). A more recent study on leukemic stem cells showed a p21-dependent cellular response that leads to reversible cell cycle arrest and DNA repair; such data clearly illustrate the oncogenic potential of p21 (33). We have shown that p21 has negative roles for tumor growth using FOXQ1-overexpressing cells with knockdown of p21 (Fig. 5D).

Recently, accumulating evidence has shown that FOX transcriptional factors are involved in VEGF regulation and angiogenesis. For example, forkhead has exhibited a positive role in mediating induction of VEGF (42–44). In the present study, we identified *VEGFA* as a candidate target gene of FOXQ1 by microarray analysis and showed that FOXQ1 increased angiogenesis *in vivo*. Interestingly, although overexpression of FOXQ1 decreases cellular proliferation *in vitro*, it enhances tumorigenicity and tumor growth *in vivo*. We consider that this discrepancy can be explained by these angiogenic and antiapoptotic effects of FOXQ1 contribute to enhanced tumor growth *in vivo*, although p21 negatively functions.

We showed that the overexpression of FOXQ1 inhibited doxorubicin-induced and camptothecin-induced apoptosis in p53-inactivated cancer cells. Therefore, we speculated that FOXQ1 might be a new determinant factor of resistance to drug-induced apoptosis and might represent a poor prognostic factor for CRC patients.

In conclusion, FOXQ1 is markedly overexpressed in CRC and enhances tumorigenicity and tumor growth *in vivo*. We have elucidated a biological function of FOXQ1, which directly upregulates p21 transcription and promotes angiogenesis and antiapoptosis. Our findings support FOXQ1

as a new member of the cancer-related FOX family in cancer cells.

Disclosure of Potential Conflicts of Interest

No potential conflicts of interest were disclosed.

Acknowledgments

We thank Dr. Richard Simon and Dr. Amy Peng for providing us with the BRB ArrayTools software. This free software was very useful and has been developed for user-friendly applications. We also thank Eiko Honda and Shinji Kurashimo for technical assistance.

Grant Support

Third-Term Comprehensive 2nd term of the 10-Year Strategy for Cancer Control, the program for the promotion of Fundamental Studies in Health Sciences of the National Institute of Biomedical Innovation, Scientific Research from the Ministry of Education, Culture, Sports, Science and Technology of Japan grant-in-aid, and Research Resident Fellowship from the Foundation of Promotion of Cancer Research in Japan (H. Kaneda).

The costs of publication of this article were defrayed in part by the payment of page charges. This article must therefore be hereby marked *advertisement* in accordance with 18 U.S.C. Section 1734 solely to indicate this fact.

Received 06/18/2009; revised 10/28/2009; accepted 12/01/2009; published OnlineFirst 02/09/2010.

References

1. Jonsson H, Peng SL. Forkhead transcription factors in immunology. Cell Mol Life Sci 2005;62:397–409.
2. Carlsson P, Mahlapuu M. Forkhead transcription factors: key players in development and metabolism. Dev Biol 2002;250:1–23.
3. Tran H, Brunet A, Griffith EC, Greenberg ME. The many forks in FOXO's road. Sci STKE 2003;2003:RE5.
4. Overdier DG, Porcella A, Costa RH. The DNA-binding specificity of the hepatocyte nuclear factor 3/forkhead domain is influenced by amino-acid residues adjacent to the recognition helix. Mol Cell Biol 1994;14:2755–66.
5. Hoggatt AM, Kriegel AM, Smith AF, Herring BP. Hepatocyte nuclear factor-3 homologue 1 (HFH-1) represses transcription of smooth muscle-specific genes. J Biol Chem 2000;275:31162–70.
6. Martinez-Ceballos E, Chambon P, Gudas LJ. Differences in gene expression between wild type and Hoxa1 knockout embryonic stem cells after retinoic acid treatment or leukemia inhibitory factor (LIF) removal. J Biol Chem 2005;280:16484–98.
7. Hong HK, Noveroske JK, Headon DJ, et al. The winged helix/forkhead transcription factor Foxq1 regulates differentiation of hair in satin mice. Genesis 2001;29:163–71.
8. Potter CS, Peterson RL, Barth JL, et al. Evidence that the satin hair mutant gene Foxq1 is among multiple and functionally diverse regulatory targets for Hoxc13 during hair follicle differentiation. J Biol Chem 2006;281:29245–55.
9. Goering W, Adham IM, Pasche B, et al. Impairment of gastric acid secretion and increase of embryonic lethality in Foxq1-deficient mice. Cytogenet Genome Res 2008;121:88–95.
10. Verzi MP, Khan AH, Ito S, Shivdasani RA. Transcription factor foxq1 controls mucin gene expression and granule content in mouse stomach surface mucous cells. Gastroenterology 2008; 135:591–600.
11. Harper JW, Adami GR, Wei N, Keyomarsi K, Elledge SJ. The p21 Cdk-interacting protein Cip1 is a potent inhibitor of G_1 cyclin-dependent kinases. Cell 1993;75:805–16.
12. Xiong Y, Hannon GJ, Zhang H, Casso D, Kobayashi R, Beach D. p21 is a universal inhibitor of cyclin kinases. Nature 1993;366:701–4.
13. el-Deiry WS, Tokino T, Velculescu VE, et al. WAF1, a potential mediator of p53 tumor suppression. Cell 1993;75:817–25.
14. Brugarolas J, Moberg K, Boyd SD, Taya Y, Jacks T, Lees JA. Inhibition of cyclin-dependent kinase 2 by p21 is necessary for retinoblastoma protein-mediated G_1 arrest after γ-irradiation. Proc Natl Acad Sci U S A 1999;96:1002–7.
15. Sherr CJ, Roberts JM. CDK inhibitors: positive and negative regulators of G_1-phase progression. Genes Dev 1999;13:1501–12.
16. Garner E, Raj K. Protective mechanisms of p53-21-pRb proteins against DNA damage-induced cell death. Cell Cycle 2008;7:277–82.
17. Maki CG, Howley PM. Ubiquitination of p53 and p21 is differentially affected by ionizing and UV radiation. Mol Cell Biol 1997;17:355–63.
18. Gartel AL, Tyner AL. Transcriptional regulation of the p21((WAF1/CIP1)) gene. Exp Cell Res 1999;246:280–9.
19. Gartel AL, Tyner AL. The role of the cyclin-dependent kinase inhibitor p21 in apoptosis. Mol Cancer Ther 2002;1:639–49.
20. Yamanaka R, Arao T, Yajima N, et al. Identification of expressed genes characterizing long-term survival in malignant glioma patients. Oncogene 2006;25:5994–6002.
21. Tanaka K, Arao T, Maegawa M, et al. SRPX2 is overexpressed in gastric cancer and promotes cellular migration and adhesion. Int J Cancer 2009;124:1072–80.
22. Takeda M, Arao T, Yokote H, et al. AZD2171 shows potent antitumor activity against gastric cancer over-expressing fibroblast growth factor receptor 2/keratinocyte growth factor receptor. Clin Cancer Res 2007;13:3051–7.
23. United Kingdom Co-ordinating Committee on Cancer Research (UKCCCR). Guidelines for the Welfare of Animals in Experimental Neoplasia (Second Edition). Br J Cancer 1998;77:1–10.
24. Iwasa T, Okamoto I, Suzuki M, et al. Inhibition of insulin-like growth factor 1 receptor by CP-751,871 radiosensitizes non-small cell lung cancer cells. Clin Cancer Res 2009;15:5117–25.
25. Shimada K, Nakamura M, Anai S, et al. A novel human AlkB homologue, ALKBH8, contributes to human bladder cancer progression. Cancer Res 2009;69:3157–64.
26. Igarashi T, Izumi H, Uchiumi T, et al. Clock and ATF4 transcription system regulates drug resistance in human cancer cell lines. Oncogene 2007;26:4749–60.
27. Bieller A, Pasche B, Frank S, et al. Isolation and characterization of the human forkhead gene FOXQ1. DNA Cell Biol 2001;20:555–61.
28. Datto MB, Yu Y, Wang XF. Functional analysis of the transforming growth factor β responsive elements in the WAF1/Cip1/p21 promoter. J Biol Chem 1995;270:28623–8.
29. Mahyar-Roemer M, Roemer K. p21 Waf1/Cip1 can protect human colon carcinoma cells against p53-dependent and p53-independent apoptosis induced by natural chemopreventive and therapeutic agents. Oncogene 2001;20:3387–98.
30. Mukherjee S, Conrad SE. c-Myc suppresses p21WAF1/CIP1 expression during estrogen signaling and antiestrogen resistance in human breast cancer cells. J Biol Chem 2005;280:17617–25.
31. Seoane J, Le HV, Massague J. Myc suppression of the p21(Cip1) Cdk inhibitor influences the outcome of the p53 response to DNA damage. Nature 2002;419:729–34.
32. Rowland BD, Peeper DS. KLF4, p21 and context-dependent opposing forces in cancer. Nat Rev Cancer 2006;6:11–23.
33. Viale A, De Franco F, Orleth A, et al. Cell-cycle restriction limits DNA damage and maintains self-renewal of leukaemia stem cells. Nature 2009;457:51–6.
34. Brunet A, Bonni A, Zigmond MJ, et al. Akt promotes cell survival by phosphorylating and inhibiting a Forkhead transcription factor. Cell 1999;96:857–68.
35. Paik JH, Kollipara R, Chu G, et al. FoxOs are lineage-restricted redundant tumor suppressors and regulate endothelial cell homeostasis. Cell 2007;128:309–23.
36. Myatt SS, Lam EW. The emerging roles of forkhead box (Fox) proteins in cancer. Nat Rev Cancer 2007;7:847–59.
37. Kalin TV, Wang IC, Ackerson TJ, et al. Increased levels of the FoxM1 transcription factor accelerate development and progression of prostate carcinomas in both TRAMP and LADY transgenic mice. Cancer Res 2006;66:1712–20.

38. Seoane J, Le HV, Shen L, Anderson SA, Massague J. Integration of Smad and forkhead pathways in the control of neuroepithelial and glioblastoma cell proliferation. Cell 2004;117:211–23.
39. Dong Y, Chi SL, Borowsky AD, Fan Y, Weiss RH. Cytosolic p21Waf1/Cip1 increases cell cycle transit in vascular smooth muscle cells. Cell Signal 2004;16:263–9.
40. Dupont J, Karas M, LeRoith D. The cyclin-dependent kinase inhibitor p21CIP/WAF is a positive regulator of insulin-like growth factor I-induced cell proliferation in MCF-7 human breast cancer cells. J Biol Chem 2003;278:37256–64.
41. Zhang C, Kavurma MM, Lai A, Khachigian LM. Ets-1 protects vascular smooth muscle cells from undergoing apoptosis by activating p21WAF1/Cip1: ETS-1 regulates basal and inducible p21WAF1/Cip: ETS-1 regulates basal and inducible p21WAF1/Cip1 transcription via distinct *cis*-acting elements in the p21WAF/Cip1 promoter. J Biol Chem 2003;278:27903–9.
42. Banham AH, Boddy J, Launchbury R, et al. Expression of the forkhead transcription factor FOXP1 is associated both with hypoxia inducible factors (HIFs) and the androgen receptor in prostate cancer but is not directly regulated by androgens or hypoxia. Prostate 2007;67:1091–8.
43. Furuyama T, Kitayama K, Shimoda Y, et al. Abnormal angiogenesis in Foxo1 (Fkhr)-deficient mice. J Biol Chem 2004;279:34741–9.
44. Gupta S, Joshi K, Wig JD, Arora SK. Intratumoral FOXP3 expression in infiltrating breast carcinoma: its association with clinicopathologic parameters and angiogenesis. Acta Oncol 2007;46:792–7.

Published Ahead of Print on April 12, 2010 as 10.1200/JCO.2009.26.5496
The latest version is at http://jco.ascopubs.org/cgi/doi/10.1200/JCO.2009.26.5496

Successful Treatment With Erlotinib After Gefitinib-Related Severe Hepatotoxicity

A 66-year-old nonsmoking woman presented with enlarged left supraclavicular lymph nodes. She had no history of liver disease, alcohol intake, or hepatitis. Baseline blood tests showed cell counts, electrolytes, as well as renal and liver function to be normal. She had not previously received medication for her condition. A chest x-ray revealed a nodular shadow in the right upper lung field. A computed tomography scan of the chest confirmed a solitary spiculated lesion in the right upper lung lobe, disseminated nodules in the interlobar fissures, and multiple pulmonary nodules. Core biopsy of left supraclavicular lymph nodes revealed adenocarcinoma, consistent with metastasis from the primary non–small-cell lung carcinoma. Mutation analysis of lung cancer specimens obtained before first-line chemotherapy showed the presence of an exon 19 deletion of the epidermal growth factor receptor gene, and gefitinib was administered orally at a dose of 250 mg once daily. Eight weeks after the initiation of treatment, computed tomography revealed marked tumor shrinkage, which was categorized as a partial response. After 13 weeks of gefitinib treatment, laboratory investigations showed a substantial increase in serum transaminase levels (AST of 84 U/L, compared with a normal range of lower than 40; ALT of 181 U/L, compared with a normal range of lower than 35; Fig 1). Initiation of treatment with ursodeoxycholic acid and ammonium glycyrrhizate resulted in a gradual decrease in transaminase levels (to values of 31 U/L and 35 U/L for AST and ALT, respectively; Fig 1). Thirty-six weeks after the initiation of daily gefitinib administration, the transaminase levels of the proband had begun to increase again, reaching a pronounced high of 599 U/L for AST and 1,011 U/L for ALT at 37 weeks (Fig 1). Gefitinib treatment was discontinued at 36 weeks. The patient had taken no other medications or supplements, and an abdominal ultrasound revealed a normal liver with no other substantial abnormalities. A drug lymphocyte stimulation test yielded a strong positive result for gefitinib, suggesting that the hepatitis of the proband was attributable to drug allergy rather than to dose-dependent toxicity. We therefore concluded that gefitinib should not be administered further at any schedule in this patient. In the 7 weeks after gefitinib withdrawal, the patient's liver function normalized but her lung cancer progressed slightly. We initiated treatment with erlotinib accompanied by careful monitoring of liver function, and the patient has continued daily oral erlotinib (150 mg) for 15 weeks with no evidence of increased hepatic toxicity or disease progression.

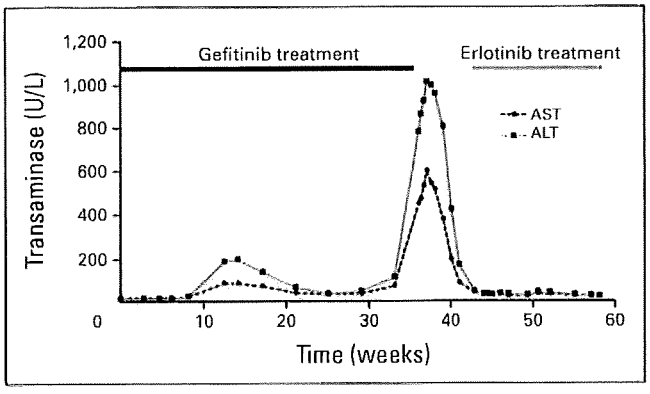

Fig 1.

Gefitinib-induced hepatitis has received little attention to date, even though phase I trials revealed hepatotoxicity as a dose-limiting toxicity of the drug and the Iressa Dose Evaluation in Advanced Lung Cancer (IDEAL 1) trial showed that 2% of patients receiving gefitinib alone at a dose of 250 mg per day developed elevations of hepatic enzymes of grade 3 or 4 that necessitated cessation of treatment.[1] Exploration of new strategies for management of gefitinib-induced severe hepatotoxicity is thus warranted. Resumption of gefitinib treatment after its discontinuation as a result of the development of drug-induced hepatitis has been reported in three cases. However, gefitinib was again discontinued because of repeated elevation of serum transaminase levels in two of three cases[2,3]; the other case showed that an intermittent schedule of gefitinib administration (250 mg/d every 5 days) reduced hepatotoxicity, although the response had been maintained for only 8 weeks at the time of report submission.[4] These findings prompted us not to recommend resumption of gefitinib treatment after the development of severe hepatotoxicity in this patient. Erlotinib acts in a manner similar to that of gefitinib and has been shown to provide clinical benefit in patients with tumors positive for epidermal growth factor receptor gene mutations. We thus treated the proband of this study with erlotinib (150 mg once daily) as an alternative to gefitinib after discontinuation of the latter drug.

With regard to the toxicity profiles of gefitinib and erlotinib, it is important to clarify the mechanism responsible for drug-induced hepatotoxicity. Gefitinib and erlotinib share a common chemical backbone structure and exhibit similar disposition characteristics in humans after oral administration. They manifest similar oral bioavailabilities and both undergo extensive metabolism primarily by cytochrome P450 3A4, with more than 80% of the administered dose being found in feces.[5,6] Administration of erlotinib at the maximum-tolerated dose and approved dose of 150 mg once daily resulted in a steady-state plasma trough concentration that was approximately 3.5 times that for gefitinib administered at the recommended dose (approximately one third of the maximum tolerated dose) of 250 mg once daily.[7,8] This patient received no medications that influence the pharmacokinetics of gefitinib or erlotinib, suggesting that the plasma concentration of gefitinib per se did not give rise to the drug-induced hepatotoxicity, although the toxicity of gefitinib has not been directly compared with that of erlotinib alone. Instead, the positive result of the drug lymphocyte stimulation test supports a diagnosis of gefitinib-induced allergic hepatitis. Erlotinib and gefitinib share a

4-anilinoquinazoline base structure, but differ in the substituents attached to the quinazoline and anilino rings. Minor differences in the chemical structures of these compounds may thus influence hepatotoxicity. In conclusion, erlotinib is an effective and well-tolerated treatment option for patients for whom gefitinib has been discontinued because of severe hepatotoxicity. Clinical trials to evaluate the administration of erlotinib after severe hepatotoxicity induced by daily administration of gefitinib are warranted.

Masayuki Takeda and Isamu Okamoto
Department of Medical Oncology, Kinki University School of Medicine, Osaka, Japan

Masahiro Fukuoka
Department of Medical Oncology, Kinki University School of Medicine, Sakai Hospital, Osaka, Japan

Kazuhiko Nakagawa
Department of Medical Oncology, Kinki University School of Medicine, Osaka, Japan

AUTHORS' DISCLOSURES OF POTENTIAL CONFLICTS OF INTEREST
The author(s) indicated no potential conflicts of interest.

REFERENCES

1. Fukuoka M, Yano S, Giaccone G, et al: Multi-institutional randomized phase II trial of gefitinib for previously treated patients with advanced non-small-cell lung cancer (The IDEAL 1 trial). J Clin Oncol 21:2237-2246, 2003
2. Ho C, Davis J, Anderson F, et al: Side effects related to cancer treatment: CASE 1. Hepatitis following treatment with gefitinib. J Clin Oncol 23:8531-8533, 2005
3. Carlini P, Papaldo P, Fabi A, et al: Liver toxicity after treatment with gefitinib and anastrozole: Drug-drug interactions through cytochrome P450? J Clin Oncol 24:e60-e61, 2006
4. Seki N, Uematsu K, Shibakuki R, et al: Promising new treatment schedule for gefitinib responders after severe hepatotoxicity with daily administration. J Clin Oncol 24:3213-3214, 2006; author reply 24:3214-3215, 2006
5. Ling J, Johnson KA, Miao Z, et al: Metabolism and excretion of erlotinib, a small molecule inhibitor of epidermal growth factor receptor tyrosine kinase, in healthy male volunteers. Drug Metab Dispos 34:420-426, 2006
6. McKillop D, McCormick AD, Millar A, et al: Cytochrome P450-dependent metabolism of gefitinib. Xenobiotica 35:39-50, 2005
7. Li J, Karlsson MO, Brahmer J, et al: CYP3A phenotyping approach to predict systemic exposure to EGFR tyrosine kinase inhibitors. J Natl Cancer Inst 98:1714-1723, 2006
8. Tan AR, Yang X, Hewitt SM, et al: Evaluation of biologic end points and pharmacokinetics in patients with metastatic breast cancer after treatment with erlotinib, an epidermal growth factor receptor tyrosine kinase inhibitor. J Clin Oncol 22:3080-3090, 2004

DOI: 10.1200/JCO.2009.26.5496; published online ahead of print at www.jco.org on April 12, 2010

Annals of Oncology Advance Access published January 11, 2010

original article

Annals of Oncology
doi:10.1093/annonc/mdp588

Is response rate increment obtained by molecular targeted agents related to survival benefit in the phase III trials of advanced cancer?

K. Tsujino[1]*, J. Shiraishi[2], T. Tsuji[3], T. Kurata[4], T. Kawaguchi[3], A. Kubo[5] & M. Takada[6]

[1]Department of Respiratory Medicine, Allergy and Rheumatic Diseases, Osaka University Graduate School of Medicine, Suita, Osaka; [2]Department of Medical Physics, School of Health Sciences, Kumamoto University, Kumamoto; [3]Department of Internal Medicine, National Hospital Organization Kinki-chuo Chest Medical Center, Sakai, Osaka; [4]Department of Medical Oncology, Kinki University School of Medicine, Osakasayama, Osaka; [5]Division of Respiratory Medicine and Allergology, Department of Internal Medicine, Aichi Medical University School of Medicine, Aichi and [6]Department of Medical Oncology, Sakai Hospital, Kinki University School of Medicine, Sakai, Osaka, Japan

Received 11 August 2009; revised 12 November 2009; accepted 19 November 2009

Background: It remains unclear whether response rate (RR) is related to survival benefit in phase III trials of advanced cancer treated with molecular targeted agents (MTA) in combination with standard therapies.

Materials and methods: We carried out a systematic search of PubMed for randomized phase III trials of four solid tumors examining the efficacy of MTA when added to a standard therapy. We examined whether there were any associations between RR increment obtained by the addition of targeted agents (ΔRR) and survival benefit in phase III trials.

Results: We identified 26 phase III trials of MTA with a total of 21 156 patients and 29 experimental arms of MTA. Studies which showed significant survival benefit had higher ΔRR compared with those which did not show significant benefit. In the receiver operating characteristic curve analysis, using a 7% gain as threshold value for ΔRR allowed assessment of survival benefit with high sensitivity and specificity. There were also significant relationships between ΔRR and hazard ratios for overall survival and progression-free survival in the linear regression analysis.

Conclusion: RR increment obtained by the addition of MTA to a standard therapy may be useful to predict survival benefit in clinical phase III trials of advanced cancer.

Key words: molecular targeted agents, response rate, survival benefit

original article

introduction

In recent years, targeted therapies have become an important modality in cancer treatment. A growing number of new agents targeting molecular pathways are tested individually or in combination with standard treatments in clinical trials. Gaining higher response rate (RR) has usually been determined as a primary end point in phase II studies evaluating the efficacy of new cytotoxic drugs [1]. However, molecular targeted agents (MTA) appear to be different from cytotoxic agents in their tumor-killing mechanism, and therefore, RR might not be an appropriate end point for phase II or screening studies of MTA [2, 3]. Of course, demonstrating an association of RR and survival in phase III trials does not imply that RR can be used instead of survival for registrational trials. The latter use of a surrogate requires a stronger relationship such as was shown by Sargent et al. [4] and used in the decision to approve oxaliplatin for adjuvant colon cancer.

We have recently indicated that RR could be a surrogate marker for survival in the clinical trials of non-small-cell lung cancer treated with gefitinib or erlotinib [5]. However, as noted above, to enable registrational trials to use RR instead of survival would require a dataset indicating that a surrogate threshold effect (STE) was exceeded by the RR found in the particular registrational trials. El-Maraghi and Eisenhauer [6] reported that objective RR seemed to be a useful end point for new targeted agents because, in their review, its observation was predictive of regulatory approval for US Food and Drug Administration. However, their analyses were limited to trials of single agents, and the authors did not discuss if their conclusions were valid for combinations of MTA with cytotoxics or others.

It is not easy to predict the effectiveness of combination therapies from results of their single-agent studies [7]. Consequently, not only single-agent phase II studies but also combination phase II studies seem to be necessary to investigate whether there is enough evidence of benefit of the new combination to warrant a phase III combination trial. Therefore, it is crucial to identify appropriate end points of combination phase II studies.

*Correspondence to: Dr K. Tsujino, Department of Respiratory Medicine, Allergy and Rheumatic Diseases, Osaka University Graduate School of Medicine, 2-2 Yamadaoka, Suita-shi, Osaka 565-0871, Japan. Tel: +81-6-6879-3831; Fax: +81-6-6879-3839; E-mail: ktujino@imed3.med.osaka-u.ac.jp

The purpose of this study is to investigate through a systematic review of publications whether RR is useful to predict survival benefit in phase III trials of advanced cancer treated with MTA in combination with standard therapies. To our knowledge, this is the first analysis investigating the relationships between RR and survival benefit in phase III trials of MTA in combination with standard therapies. As many targeted agents continue to be used in combination with established chemotherapies, it is important to discuss this issue considering novel agents yet to be developed.

materials and methods

literature search and data extraction

We carried out a systematic search of PubMed for randomized phase III trials examining the efficacy of MTA when added to a standard therapy. We targeted randomized phase III trials evaluating survival benefit which compared a combination therapy of a standard therapy and MTA with the standard therapy alone or with a placebo. All trials that had been reported by 31 May 2009, were targeted. Biotherapy such as immune therapy or hormonal therapy was not considered as a molecular targeted therapy in our analyses. We defined four common solid cancer types (lung, colorectal, breast, and renal cell carcinoma) on which to focus.

Systematic search was carried out using the key words lung cancer, colorectal cancer, breast cancer, and renal cell carcinoma. All searches were limited to 'English language' and 'clinical trial, phase III' or 'randomized controlled trial'. Retrospective subgroup analyses of phase III trials were not included. Trials involving radiation therapy or using MTA as adjuvant, neoadjuvant, or consolidation therapies were excluded from our analysis.

For each trial, data on sample size, primary and secondary end points, RR, overall survival (OS), progression-free survival (PFS), time to progression (TTP), types of MTA, and therapy regimens were collected. Also investigated in each study was whether statistically significant benefit of OS or PFS was observed in an experimental arm of MTA compared with a control arm. When available, hazard ratios (HRs) for OS and PFS were collected. We also recorded data of study designs on response evaluation to assess heterogeneity across studies.

All phase III studies were retrieved independently by two investigators (KT and TT) to assess the reliability of data extraction.

statistical analysis

For each trial, the difference in RR (ΔRR) was calculated as the estimate in the experimental arm minus the estimate in the control arm. Using Student's t-test, we examined whether there are any differences in the distribution of ΔRR between trial arms which showed survival benefit and those which did not show survival benefit. In addition, we calculated the area under receiver operating characteristic (ROC) curves (AUCs) to examine the accuracy of ΔRR to predict survival benefit in phase III studies. A binormal ROC curve was fitted to ΔRR for positive and negative groups classified by the presence of significant benefit in OS or PFS. By use of the actual value of ΔRR, a computer program (ROCKIT program [8], kindly provided by Metz, The University of Chicago) was employed for estimating binormal ROC curves as well as the AUC value and its 95% confidence interval.

Linear regression analysis was carried out to evaluate the correlation between ΔRR and HR of OS or PFS. In this model, the prediction bands were calculated and the STE was determined by the intersection of the upper prediction band and the HR = 1 line. This method estimates the threshold level of a surrogate needed in a new individual clinical trial to predict gain in the target outcome [9]. Concerning the heterogeneity of the tumor types, linear regression analysis was also carried out limited to only lung cancer studies and colorectal cancer studies. Given the small number of studies for the other tumor types, insufficient data were available to carry out statistical analysis. Linear regression analysis was also employed to evaluate the correlation between HR of PFS and that of OS.

A P value <0.05 was considered statistically significant, and all reported P values were two sided. All statistical analyses except those of ROC were carried out using SPSS 17.0 for Windows (SPSS, Inc., Chicago, IL).

results

study characteristics

We identified 26 phase III trials of MTA with a total of 21,156 patients and 29 experimental arms of MTA in combination with standard therapy. The baseline characteristics of the 26 trials are shown in Table 1 [10–35]. There were 10 lung cancer studies, 7 colon cancer studies, 6 breast cancer studies, and 3 renal cell carcinoma studies.

The sample size of each arm with MTA ranged from 228 to 1401, with a median sample size of 773 patients. Four trials included death in the definition of TTP, and therefore, they were calculated as PFS in our analysis. Twenty-five study arms with MTA contained mature data of PFS, and 12 of them reported statistically significant benefits of experimental arms (arms with MTA) compared with control arms. In contrast, 25 study arms with MTA contained mature data of OS, and 5 of them reported statistically significant benefits. RR was reported in all included studies, and ΔRR ranged from −7.9% to 20.0% (median: 5.5%).

A primary end point and data on response evaluation in each study are summarized in supplemental Table S1 (available at *Annals of Oncology* online). In the trials we used, the primary end point most frequently used was OS, followed by PFS. In addition, there appeared to be some differences among each study in the methods of response evaluation.

validity of regression model

For all regression analyses, none of the tests for normality of error and heteroscedasticity were statistically significant.

RR and survival benefit

Studies which showed significant benefit in OS had higher ΔRR compared with those which did not show significant benefit in OS ($P = 0.002$, Figure 1A). Similarly, studies with significant benefit in PFS had higher ΔRR compared with those without significant benefit in PFS ($P < 0.001$, Figure 1B). In an ROC analysis, the AUC value and its 95% confidence interval for predicting the presence of significant benefit in OS by ΔRR were 0.903 (0.670–0.985) and that for predicting the presence of significant benefit in PFS by ΔRR were 0.910 (0.730–0.985) (Figure 1C and D). Both performed significantly better than random guessing of survival benefit. Using a 7% gain as threshold value for ΔRR allowed assessment of survival benefit with a sensitivity of 91% and a specificity of 70% in OS and with a sensitivity of 84% and a specificity of 85% in PFS.

Similar findings were observed in subgroup analyses of individual cancer types. A 7% gain of ΔRR significantly correlated with the presence of survival benefit in phase III study in each cancer type (supplemental Table S2, available at *Annals of Oncology* online). Notably, all lung cancer studies

Table 1. Trials included in the analysis ($N = 26$)

Cancer type/agents	Target	Drug type	Trials	Control arms	Placebo controlled	No. of patients	Primary end point
Lung cancer							
Gefitinib	EGFR	SM	Giaccone et al., 2004 [10]	CDDP + GEM	No	1093	OS
			Herbst et al., 2004 [11]	CBDCA + PTX	No	1037	OS
Erlotinib	EGFR	SM	Herbst et al., 2005 [12]	CBDCA + PTX	No	1079	OS
			Gatzemeier et al., 2007 [13]	CDDP + GEM	No	1159	OS
Bevacizumab	VEGF	AB	Sandler et al., 2006 [14]	CBDCA + PTX	No	878	OS
			Reck et al., 2009 [15]	CDDP + GEM	Yes	1043	PFS
Cetuximab	EGFR	AB	Pirker et al., 2009 [16]	CDDP + VNR	No	1125	OS
Prinomastat	Matrix metalloproteinase	SM	Bissett et al., 2005 [17]	CDDP + GEM	Yes	362	OS
BMS-275291	Matrix metalloproteinase	SM	Leighl et al., 2005 [18]	CBDCA + PTX	Yes	774	OS
Aprinocarsen	Protein kinase C alpha	AS	Paz-Ares et al., 2006 [19]	CDDP + GEM	No	670	OS
Colorectal cancer							
Bevacizumab	VEGF	AB	Hurwitz et al., 2004 [20]	FOLFIRI	Yes	813	OS
			Giantonio et al., 2007 [21]	FOLFOX	No	577	OS
			Saltz et al., 2008 [22]	FOLFOX or XELOX	Yes	1401	PFS
Panitumumab	EGFR	AB	Hecht et al., 2009 [23]	OX-CT or Iri-CT + Bev	No	1053	PFS
Cetuximab	EGFR	AB	Sobrero et al., 2008 [24]	Irinotecan	No	1298	OS
			Tol et al., 2009 [25]	XELOX + Bev	No	755	PFS
			Van Cutsem et al., 2009 [26]	FOLFIRI	No	1198	PFS
Breast cancer							
Trastuzumab	HER-2	AB	Slamon et al., 2001 [27]	Standard chemotherapy[a]	No	469	TTP
			Seidman et al., 2008 [28]	PTX	No	228	RR
Lapatinib	EGFR/HER-2	SM	Geyer et al., 2006 [29]	Capecitabine	No	324	TTP
			Di Leo et al., 2008 [30]	PTX	Yes	579	TTP
Bevacizumab	VEGF	AB	Miller et al., 2005 [31]	Capecitabine	No	462	PFS
			Miller et al., 2007 [32]	PTX	No	772	PFS
Renal cell carcinoma							
Bevacizumab	VEGF	AB	Escudier et al., 2007 [33]	Interferon alfa	Yes	649	OS
			Rini et al., 2008 [34]	Interferon alfa	No	732	OS
Temsirolimus	mTOR	SM	Hudes et al., 2007 [35]	Interferon alfa	No	626	OS

EGFR, epidermal growth factor receptor; SM, small molecule; CDDP, cisplatin; GEM, gemcitabine; OS, overall survival; CBDCA, carboplatin; PTX, paclitaxel; VEGF, vascular endothelial growth factor; AB, antibody; PFS, progression-free survival; VNR, vinorelbine; AS, antisense oligonucleotide; FOLFIRI, irinotecan + 5-fluorouracil + leucovorin; XELOX, capecitabine + oxaliplatin; OX-CT, oxaliplatin-based chemotherapy; Iri-CT, irinotecan-based chemotherapy; Bev, bevacizumab; HER-2, human epidermal growth factor receptor-2; TTP, time to progression; RR, response rate; mTOR, mammalian target of rapamycin.

[a]Doxorubicin or epirubicin plus cyclophosphamide for patients who had never received an anthracycline or PTX for patients who had received adjuvant anthracycline.

with ΔRR no less than 7% showed significant benefit in at least either of OS or of PFS, whereas no lung cancer study with ΔRR <7% showed significant benefit in any survival.

RR and survival improvement

Eighteen studies with 18 arms for OS and 17 studies with 18 arms for PFS had data of HRs. There were significant relationships between ΔRR and HR for OS or PFS on unweighted linear regression analysis ($P = 0.002$ and 0.001, $R^2 = 0.47$ and 0.50, respectively, Figure 2A and B). The STE levels of ΔRR calculated from prediction bands were 21% for OS and 15% for PFS. The regression analysis weighted for trial size showed similar results (data not shown).

Linear regression analyses were also carried out limited to lung or colorectal cancer studies (Figure 2). Despite the number of evaluable studies being small, ΔRR in lung cancer studies showed strong relationships with both HR for OS and that for PFS. Similarly, a significant relationship was observed between ΔRR and HR for PFS in colorectal cancer studies.

PFS and OS

Only 14 studies reported both HR of PFS and that of OS. In unweighted regression analysis, HR of PFS significantly correlated with that of OS ($P < 0.001$, $R^2 = 0.69$; supplemental Figure S1, available at *Annals of Oncology* online). The regression analysis weighted for trial size showed similar results (data not shown).

discussion

Possible interactions in therapeutic effects of MTA and standard therapies have made it difficult to predict the relation between clinical response and survival benefit. Our analysis showed, on average, that the addition of MTA to standard

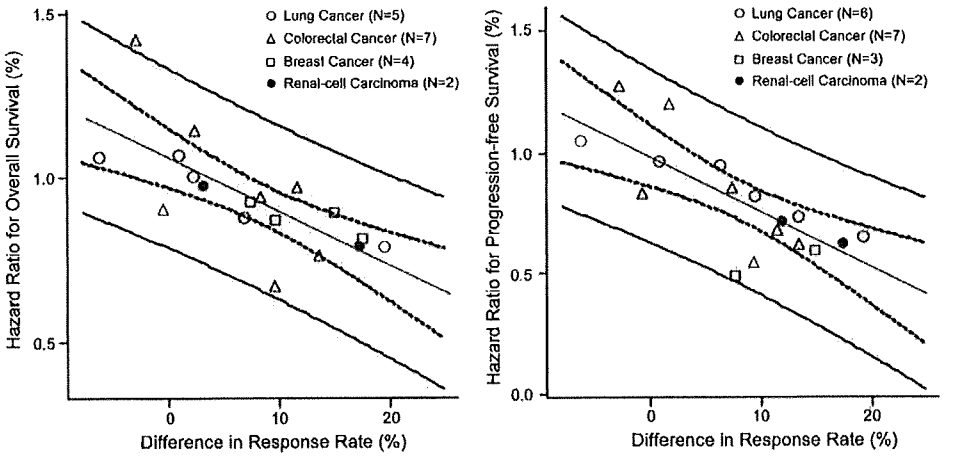

Cancer Type	Coefficient	R^2	P-Value
Lung Cancer	-0.011	0.84	0.030
Colorectal Cancer	-0.029	0.51	0.072
All	-0.016	0.47	0.002

Cancer Type	Coefficient	R^2	P-Value
Lung Cancer	-0.015	0.94	0.002
Colorectal Cancer	-0.037	0.65	0.029
All	-0.022	0.50	0.001

Figure 2. (A) Correlation between difference in RR and HR for overall survival. (B) Correlation between difference in RR and HR for progression-free survival. The linear regression line is shown (the central straight line). Dotted inner lines are the 95% confidence bands and bold outer lines are the 95% prediction bands. RR, response rate; HR, hazard ratio.

for the development of drug combinations [39], there may have been a corresponding increase in the use of PFS as a primary end point of phase II studies. In our analysis, HR of PFS appeared to be closely related to that of OS, and we do agree that PFS may be an appropriate predictor for OS, at least in phase III trials. However, small randomized trials bring with them unavoidable issues such as high false-positive and -negative rates and unstable *P* values [40]. In particular, PFS has often been used as a primary end point in recent phase III studies, and therefore, the use of PFS as a single end point for a randomized phase II trial may render this an underpowered phase III trial. We believe that the use of RR, which is standardized and easily applicable to multicenter trials, in addition to PFS as an end point for randomized phase II studies could reduce these problems and give us further information which leads to successful phase III trials of MTA in combination with standard therapies. However, this interpretation requires a caution. We do not mean that RR can be used as a surrogate for survival in phase III trials. It requires a trial to yield ΔRR above the STE level of 21% or 15%, which may be a difficult test for a new drug. RR should be used as one of the screening measures in phase II studies, and thereafter, the presence of survival benefits should be investigated again in subsequent phase III studies. Our analysis has several limitations to be noted.

First, we have not covered a comprehensive review of all clinical trials including unpublished ones. Because negative studies would eventually stand a lower chance of being published, this publication bias can lead to an overestimation of treatment effect of targeted agents.

Second, the heterogeneity of study design in each trial may affect our results. The method of evaluating response is not exactly the same in each study (supplemental Table S1, available at *Annals of Oncology* online), and RR and PFS can be affected by these differences. Moreover, the method of sample size calculation is not the same across studies. Significance of survival benefit could be affected in part by the statistical property of such designs. In addition, there is a caution if we use the data of RRs in phase II studies. RRs observed in phase III studies may tend to be lower than those in phase II studies [41, 42].

Finally, there were four different cancer types included in our analysis. Biology and sensitivity to drugs may be different among each cancer type. These heterogeneities may influence the relation between response and survival benefit. However, there appeared to be no major differences among four cancer types in cut-off points of ΔRR predicting survival benefit. In addition, similar findings were observed in the linear regression analysis even if limited to lung cancer studies. Therefore, we believe our conclusion could be validated at least for lung studies.

In conclusion, our review indicated that RR increment obtained by the addition of MTA to a standard therapy was associated to survival benefit in clinical phase III trials of advanced cancer. The use of RR as an end point in screening studies of targeted agents in combination with standard therapies may help lead to successful phase III trials in terms of survival benefit, at least for lung cancer.

funding

The Osaka Medical Research Foundation for Incurable Diseases.

acknowledgements

We are grateful to Prof. Nagahiro Saijo (Department of Medical Oncology, Kinki University School of Medicine) for his critical

reading of the manuscript and his helpful comments. We thank Juri Mori for data management.

disclosure

None of the authors have any conflicts of interest associated with this study.

references

1. Parulekar WR, Eisenhauer EA. Novel endpoints and design of early clinical trials. Ann Oncol 2002; 13 (Suppl 4): 139–143.
2. Dhani N, Tu D, Sargent DJ et al. Alternate endpoints for screening phase II studies. Clin Cancer Res 2009; 15: 1873–1882.
3. Karrison TG, Maitland ML, Stadler WM, Ratain MJ. Design of phase II cancer trials using a continuous endpoint of change in tumor size: application to a study of sorafenib and erlotinib in non small-cell lung cancer. J Natl Cancer Inst 2007; 99: 1455–1461.
4. Sargent DJ, Wieand HS, Haller DG et al. Disease-free survival versus overall survival as a primary end point for adjuvant colon cancer studies: individual patient data from 20,898 patients on 18 randomized trials. J Clin Oncol 2005; 23: 8664–8670.
5. Tsujino K, Kawaguchi T, Kubo A et al. Response rate is associated with prolonged survival in patients with advanced non-small cell lung cancer treated with gefitinib or erlotinib. J Thorac Oncol 2009; 4: 994–1001.
6. El-Maraghi RH, Eisenhauer EA. Review of phase II trial designs used in studies of molecular targeted agents: outcomes and predictors of success in phase III. J Clin Oncol 2008; 26: 1346–1354.
7. Dancey JE, Chen HX. Strategies for optimizing combinations of molecularly targeted anticancer agents. Nat Rev Drug Discov 2006; 5: 649–659.
8. Metz CE, Herman BA, Shen JH. Maximum likelihood estimation of receiver operating characteristic (ROC) curves from continuously-distributed data. Stat Med 1998; 17: 1033–1053.
9. Burzykowski T, Buyse M. Surrogate threshold effect: an alternative measure for meta-analytic surrogate endpoint validation. Pharm Stat 2006; 5: 173–186.
10. Giaccone G, Herbst RS, Manegold C et al. Gefitinib in combination with gemcitabine and cisplatin in advanced non-small-cell lung cancer: a phase III trial–INTACT 1. J Clin Oncol 2004; 22: 777–784.
11. Herbst RS, Giaccone G, Schiller JH et al. Gefitinib in combination with paclitaxel and carboplatin in advanced non-small-cell lung cancer: a phase III trial–INTACT 2. J Clin Oncol 2004; 22: 785–794.
12. Herbst RS, Prager D, Hermann R et al. TRIBUTE: a phase III trial of erlotinib hydrochloride (OSI-774) combined with carboplatin and paclitaxel chemotherapy in advanced non-small-cell lung cancer. J Clin Oncol 2005; 23: 5892–5899.
13. Gatzemeier U, Pluzanska A, Szczesna A et al. Phase III study of erlotinib in combination with cisplatin and gemcitabine in advanced non-small-cell lung cancer: the tarceva lung cancer investigation trial. J Clin Oncol 2007; 25: 1545–1552.
14. Sandler A, Gray R, Perry MC et al. Paclitaxel-carboplatin alone or with bevacizumab for non-small-cell lung cancer. N Engl J Med 2006; 355: 2542–2550.
15. Reck M, von Pawel J, Zatloukal P et al. Phase III trial of cisplatin plus gemcitabine with either placebo or bevacizumab as first-line therapy for nonsquamous non-small-cell lung cancer: AVAil. J Clin Oncol 2009; 27: 1227–1234.
16. Pirker R, Pereira JR, Szczesna A et al. Cetuximab plus chemotherapy in patients with advanced non-small-cell lung cancer (FLEX): an open-label randomised phase III trial. Lancet 2009; 373: 1525–1531.
17. Bissett D, O'Byrne KJ, von Pawel J et al. Phase III study of matrix metalloproteinase inhibitor prinomastat in non-small-cell lung cancer. J Clin Oncol 2005; 23: 842–849.
18. Leighl NB, Paz-Ares L, Douillard JY et al. Randomized phase III study of matrix metalloproteinase inhibitor BMS-275291 in combination with paclitaxel and carboplatin in advanced non-small-cell lung cancer: national cancer institute of canada-clinical trials group study BR.18. J Clin Oncol 2005; 23: 2831–2839.
19. Paz-Ares L, Douillard JY, Koralewski P et al. Phase III study of gemcitabine and cisplatin with or without aprinocarsen, a protein kinase C-alpha antisense oligonucleotide, in patients with advanced-stage non-small-cell lung cancer. J Clin Oncol 2006; 24: 1428–1434.
20. Hurwitz H, Fehrenbacher L, Novotny W et al. Bevacizumab plus irinotecan, fluorouracil, and leucovorin for metastatic colorectal cancer. N Engl J Med 2004; 350: 2335–2342.
21. Giantonio BJ, Catalano PJ, Meropol NJ et al. Bevacizumab in combination with oxaliplatin, fluorouracil, and leucovorin (FOLFOX4) for previously treated metastatic colorectal cancer: results from the eastern cooperative oncology group study E3200. J Clin Oncol 2007; 25: 1539–1544.
22. Saltz LB, Clarke S, Diaz-Rubio E et al. Bevacizumab in combination with oxaliplatin-based chemotherapy as first-line therapy in metastatic colorectal cancer: a randomized phase III study. J Clin Oncol 2008; 26: 2013–2019.
23. Hecht JR, Mitchell E, Chidiac T et al. A randomized phase IIIB trial of chemotherapy, bevacizumab, and panitumumab compared with chemotherapy and bevacizumab alone for metastatic colorectal cancer. J Clin Oncol 2009; 27: 672–680.
24. Sobrero AF, Maurel J, Fehrenbacher L et al. EPIC: phase III trial of cetuximab plus irinotecan after fluoropyrimidine and oxaliplatin failure in patients with metastatic colorectal cancer. J Clin Oncol 2008; 26: 2311–2319.
25. Tol J, Koopman M, Cats A et al. Chemotherapy, bevacizumab, and cetuximab in metastatic colorectal cancer. N Engl J Med 2009; 360: 563–572.
26. Van Cutsem E, Kohne CH, Hitre E et al. Cetuximab and chemotherapy as initial treatment for metastatic colorectal cancer. N Engl J Med 2009; 360: 1408–1417.
27. Slamon DJ, Leyland-Jones B, Shak S et al. Use of chemotherapy plus a monoclonal antibody against HER2 for metastatic breast cancer that overexpresses HER2. N Engl J Med 2001; 344: 783–792.
28. Seidman AD, Berry D, Cirrincione C et al. Randomized phase III trial of weekly compared with every-3-weeks paclitaxel for metastatic breast cancer, with trastuzumab for all HER-2 overexpressors and random assignment to trastuzumab or not in HER-2 nonoverexpressors: final results of cancer and leukemia group B protocol 9840. J Clin Oncol 2008; 26: 1642–1649.
29. Geyer CE, Forster J, Lindquist D et al. Lapatinib plus capecitabine for HER2-positive advanced breast cancer. N Engl J Med 2006; 355: 2733–2743.
30. Di Leo A, Gomez HL, Aziz Z et al. Phase III, double-blind, randomized study comparing lapatinib plus paclitaxel with placebo plus paclitaxel as first-line treatment for metastatic breast cancer. J Clin Oncol 2008; 26: 5544–5552.
31. Miller KD, Chap LI, Holmes FA et al. Randomized phase III trial of capecitabine compared with bevacizumab plus capecitabine in patients with previously treated metastatic breast cancer. J Clin Oncol 2005; 23: 792–799.
32. Miller K, Wang M, Gralow J et al. Paclitaxel plus bevacizumab versus paclitaxel alone for metastatic breast cancer. N Engl J Med 2007; 357: 2666–2676.
33. Escudier B, Pluzanska A, Koralewski P et al. Bevacizumab plus interferon alfa-2a for treatment of metastatic renal cell carcinoma: a randomised, double-blind phase III trial. Lancet 2007; 370: 2103–2111.
34. Rini BI, Halabi S, Rosenberg JE et al. Bevacizumab plus interferon alfa compared with interferon alfa monotherapy in patients with metastatic renal cell carcinoma: CALGB 90206. J Clin Oncol 2008; 26: 5422–5428.
35. Hudes G, Carducci M, Tomczak P et al. Temsirolimus, interferon alfa, or both for advanced renal-cell carcinoma. N Engl J Med 2007; 356: 2271–2281.
36. Dorfman DD, Alf E Jr. Maximum likelihood estimation of parameters of signal detection theory—a direct solution. Psychometrika 1968; 33: 117–124.
37. Buyse M, Thirion P, Carlson RW et al. Relation between tumour response to first-line chemotherapy and survival in advanced colorectal cancer: a meta-analysis. Meta-Analysis Group in Cancer. Lancet 2000; 356: 373–378.
38. Tang PA, Bentzen SM, Chen EX, Siu LL. Surrogate end points for median overall survival in metastatic colorectal cancer: literature-based analysis from 39 randomized controlled trials of first-line chemotherapy. J Clin Oncol 2007; 25: 4562–4568.

original article

Annals of Oncology 21: 255–262, 2010
doi:10.1093/annonc/mdp304
Published online 24 July 2009

Association between gain-of-function mutations in *PIK3CA* and resistance to HER2-targeted agents in *HER2*-amplified breast cancer cell lines

Y. Kataoka[1], T. Mukohara[2,3]*, H. Shimada[4], N. Saijo[4], M. Hirai[1] & H. Minami[2,3]

[1]*Hospital Pharmacy;* [2]*Cancer Center, Kobe University Hospital;* [3]*Medical Oncology, Department of Medicine, Kobe University Graduate School of Medicine, Chuo-ku, Kobe and* [4]*Research Center for Innovative Oncology, National Cancer Hospital East, Kashiwa, Japan*

Received 24 April 2009; accepted 4 May 2009

Background: The mechanism of resistance to human epidermal growth factor receptor 2 (HER2)-targeted agents has not been fully understood. We investigated the influence of *PIK3CA* mutations on sensitivity to HER2-targeted agents in naturally derived breast cancer cells.

Materials and methods: We examined the effects of Calbiochem (CL)-387,785, HER2 tyrosine kinase inhibitor, and trastuzumab on cell growth and *HER2* signaling in eight breast cancer cell lines showing *HER2* amplification and trastuzumab-conditioned BT474 (BT474-TR).

Results: Four cell lines with *PIK3CA* mutations (E545K and H1047R) were more resistant to trastuzumab than the remaining four without mutations (mean percentage of control with 10 μg/ml trastuzumab: 58% versus 92%; $P = 0.010$). While *PIK3CA*-mutant cells were more resistant to CL-387,785 than *PIK3CA*-wild-type cells (mean percentage of control with 1 μM CL-387,785: 21% versus 77%; $P = 0.001$), CL-387,785 retained activity against BT474-TR. Growth inhibition by trastuzumab and CL-387,785 was more closely correlated with changes in phosphorylation of S6K (correlation coefficient, 0.811) than those of HER2, Akt, or ERK1/2. Growth of most *HER2*-amplified cells was inhibited by LY294002, regardless of *PIK3CA* genotype.

Conclusions: *PIK3CA* mutations are associated with resistance to HER2-targeted agents. PI3K inhibitors are potentially effective in overcoming trastuzumab resistance caused by *PIK3CA* mutations. S6K phosphorylation is a possibly useful pharmacodynamic marker in HER2-targeted therapy.

Key words: breast cancer, HER2, *PIK3CA*, trastuzumab

introduction

Breast cancer is the leading cause of cancer death among women worldwide, with ~1 million new cases reported each year [1, 2]. Approximately 20% of breast cancer tumors show overexpression of the HER2 protein, which is mainly caused by gene amplification. HER2 overexpression has been repeatedly identified as a poor prognostic factor [3, 4]. Trastuzumab is a humanized mAb targeting the extracellular domain of the HER2 protein. From the late 1990s, clinical studies have intensively evaluated the therapeutic roles of trastuzumab. For the treatment of HER2-overexpressing metastatic breast cancers, studies report that a combination of trastuzumab and conventional chemotherapy shows significantly higher efficacy than chemotherapy alone [5]. The use of trastuzumab has extended to the treatment of operable HER2-overexpressing breast cancer as an adjuvant or neoadjuvant [6–8]. Despite promising usefulness in clinics, a modest percentage of patients are reported to benefit from trastuzumab therapy, with response rates to trastuzumab as a single agent of ~20% [9]. In addition, even when trastuzumab therapy leads to temporary tumor shrinkage, clinical relapse is observed for the vast majority of metastatic patients. To develop adequate therapies capable of overcoming primary and secondary resistance to trastuzumab, a better understanding of the resistance mechanism is crucial.

To date, several mechanisms of primary resistance to trastuzumab have been proposed. A series of studies indicated that trastuzumab resistance is due to the truncated form of HER2, which lacks an extracellular domain to which trastuzumab is indicated to attach [10, 11]. Nagata et al. [12] demonstrated that loss of phosphatase and tensin homolog deleted on chromosome 10 (PTEN), a negative regulator of PI3K, correlates with poor response to trastuzumab. More recently, the roles of *PIK3CA* in trastuzumab resistance have been under particular investigation. Somatic mutations of *PIK3CA* were first identified in 2004 in various malignant tumors including breast cancer [13]. Subsequent studies have reported that the E545K and H1047R hotspot mutations, found

*Correspondence to: Dr T. Mukohara, Department of Medical Oncology, Kobe University Hospital, 7-5-2, Kusunoki-cho, Chuo-ku, Kobe 650-0017, Japan. Tel: +81-78-382-5825; Fax: +81-78-382-5821; E-mail: mukohara@med.kobe-u.ac.jp

on exons 9 and 20, respectively, are the most frequent types of mutation, found in 8%–40% of breast cancer tumors [13–16]. Both hotspot mutations are gain-of-function mutations which transform normal mammary epithelial cells [17, 18]. Berns et al. [19] investigated the roles of gain-of-function mutations of the *PIK3CA* gene in trastuzumab resistance by transfecting wild-type and mutant (H1047R) forms of *PIK3CA* in SKBR-3 HER2-overexpressing breast cancer cells. Results showed that compared with green fluorescent protein (GFP) control, both wild-type and mutant *PIK3CA* transfections resulted in trastuzumab resistance. Further, analysis of *PIK3CA* genotypes in tumor samples obtained from breast cancer patients having undergone trastuzumab-based therapy showed an association between the presence of *PIK3CA* hotspot mutations and shorter time to progression after therapy [19].

Tyrosine kinase inhibitors (TKIs) have also been investigated as potential agents against trastuzumab resistance [20]. A clinical study in metastatic breast cancer patients having previously experienced tumor progression under trastuzumab-based therapies showed that compared with capecitabine alone, treatment using a combination of capecitabine with lapatinib, a dual inhibitor of epidermal growth factor receptor (EGFR) and HER2 tyrosine kinase, lead to significantly longer time to progression [21]. Eichhorn et al. [22], however, demonstrated that transfection of mutant *PIK3CA* (H1047R) in BT474 HER2-overexpressing breast cancer cells resulted in resistance to lapatinib compared with parental cells. Further, results showed that resistance was overcome using NVP-BEZ235, a PI3K and mammalian target of rapamycin dual inhibitor [22].

These findings based on gene manipulations indicate that gain-of-function mutations in the *PIK3CA* gene lead to resistance to trastuzumab, as well as HER2-TKI. To our knowledge, however, these findings have not been confirmed in naturally derived breast cancer cells. Here, trastuzumab resistance due to *PIK3CA* mutations was evaluated in eight naturally derived breast cancer cell lines harboring *HER2* gene amplification. Further, possible therapeutic means to overcome primary and secondary resistance to trastuzumab were investigated, as well as potential pharmacodynamic markers correlated with the growth-inhibitory effect of HER2-targeted drugs.

materials and methods

cell culture

MCF-7, MDA-MB-361, HCC1954, MDA-MB-453, UACC893, CAMA-1, MDA-MB-435S, MDA-MB-415, ZR75-30, HCC70, MDA-MB-468, and HCC1419 cell lines were purchased from the American Type Culture Collection (Manassas, VA). BT474, SKBR-3, BT549, T47D, ZR75-1, and MDA-MB-231 cells were kindly provided by Ian Krop of the Dana-Farber Cancer Institute. Of the 18 breast cancer cell lines, eight (ZR75-30, BT474, SKBR-3, HCC1419, MDA-MB-453, MDA-MB-361, HCC1954, and UACC 893) were reported to have *HER2* gene amplification [23], with levels of PTEN protein expression equivalent to those reported in our previous study [24]. Among the *HER2*-amplified cell lines, ZR75-30, SKBR-3, and HCC1419 were reported to contain the wild-type *PIK3CA* gene and MDA-MB-453, MDA-MB-361, HCC1954, and UACC893 hotspot *PIK3CA* mutations (Table 1) [14]. BT474 was reported to contain a relatively rare type of *PIK3CA* mutation at exon 2, K111N (Table 1) [14]. MDA-MB-435S, MDA-MB-468, and MDA-MB-231 cells were maintained in Dulbecco's Modified Eagle's Medium (Cellgro; Mediatech, Inc., Herndon, CA) with 10% fetal bovine serum (FBS) (Gemini Bio-Products, Inc., Woodland, CA), 100 U/ml penicillin, 100 U/ml streptomycin, and 2 mM glutamine. The remaining cell lines were maintained in RPMI-1640 medium (Cellgro; Mediatech, Inc.) supplemented with 10% FBS, 100 U/ml penicillin, 100 U/ml streptomycin, and 2 mM glutamine. All cells were grown at 37°C in a humidified atmosphere with 5% CO_2 and were in logarithmic growth phase at initiation of the experiments.

Table 1. Genotype of *PIK3CA* in *HER2*-amplified breast cancer cell lines

Cell line	Genotype of *PIK3CA*
BT474	K111N
ZR75-30	wt
SKBR-3	wt
HCC1419	wt
MDA-MB-361	E545K
MDA-MB-453	H1047R
HCC1954	H1047R
UACC893	H1047R

wt, wild-type.

drugs

Trastuzumab was obtained from the Kobe University Hospital pharmacy. CI-387,785, a dual inhibitor of EGFR and HER2 [25], and LY294002, a PI3K inhibitor, were purchased from Calbiochem (San Diego, CA). Stock solutions were prepared in dimethyl sulfoxide (DMSO) and stored at −20°C. Before each experiment, drugs were diluted in fresh media. The final DMSO concentration was <0.1% for all experiments.

antibodies and western blotting

Cells were washed with ice-cold phosphate-buffered saline and scraped immediately after adding lysis buffer [20 mM Tris (pH 7.5), 150 mM NaCl, 10% glycerol, 1% Nonidet P-40, and 2 mM EDTA] containing protease and phosphatase inhibitors (100 mM NaF, 1 mM phenylmethylsulfonyl fluoride, 1 mM Na_3VO_4, 2 μg/ml aprotinin, and 5 μg/ml leupeptin). Lysates were centrifuged at 14 000 relative centrifugal force for 10 min. Supernatants were collected as protein extract and then separated by electrophoresis on 7.6% polyacrylamide–sodium dodecyl sulfate gels, followed by transfer to nitrocellulose membranes (Millipore Corporate Headquarters, Billerica, MA) and detection by immunoblotting using an enhanced chemiluminescence system (New England Nuclear Life Science Products, Inc., Boston, MA). The resulting signals were digitally quantified using the ImageJ software (www.nih.gov). Phospho-HER2/ErbB2 (Thr1221/1222), phospho-p70 S6 Kinase (Thr389), phospho-Akt (Ser473)(D9E), and PathScan(R) Multiplex Western Cocktail I were purchased from Cell Signaling Technology (Beverly, MA). The phospho-1/2 (pT185/pY187) antibody was purchased from Biosource International Inc. (Camarillo, CA), the c-erbb-2 antibody from Chemicon (Billerica, MA), and β-actin antibody from Sigma-Aldrich (St Louis, MO).

cell growth assay

Growth inhibition was assessed using the 3-(4,5-dimethylthiazol-2-yl)-5-(3-carboxymethoxyphenyl)-2-(4-sulfophenyl)-2H-tetrazolium (MTS) assay (Promega, Madison, WI), a colorimetric method for determining the number of viable cells based on the bioreduction of MTS to a soluble formazan product, which is detectable by spectrophotometry at a wavelength of 490 nm. Cells were diluted in 160 μl/well of maintenance cell culture media and plated in 96-well flat-bottom plates (Corning, Inc., Corning, NY). After a 96-h growth period, the number of cells required to obtain an absorbance of 1.3–2.2, the linear range of the assay, was

determined for each cell line beforehand. The number of cells per well used in the subsequent experiments were as follows: MCF-7, 2000; MDA-MB-361, 8000; HCC1954, 2500; MDA-MB-453, 7000; UACC893, 7500; CAMA-1, 6000; MDA-MB-435S, 2000; ZR75-30, 7500; HCC70, 4000; HCC1419, 8000; BT474, 3000; SKBR-3, 2500; BT549, 2000; T47D, 2500; ZR75-1, 7500; MDA-MB-415, 5000; and MDA-MB-231, 2500. At 24 h after plating, cell culture media were replaced with 10% FBS-containing media with and without trastuzumab or CL-387,785, followed by incubation for an additional 120 h. Trastuzumab and CL-387,785 concentrations ranged from 33 ng/ml to 100 μg/ml and from 3.3 nM to 10 μM, respectively. A total of 6–12 plate wells were set for each experimental point, and all experiments were carried out at least in triplicate. Data are expressed as percentage of growth relative to that of untreated control cells.

generation of *in vitro* BT474-TR

To generate a cell line resistant to trastuzumab, BT474 cells were continuously exposed to 100 μg/ml trastuzumab. To confirm the emergence of resistant clones, MTS assays were carried out every five passages after allowing cells to grow in drug-free conditions for at least 4 days. After 11 months of drug exposure, cells showed sufficient resistance (Figure 1) and were designated as BT474-TR. For controls, BT474 parental cells were concomitantly maintained without trastuzumab, and drug sensitivity was compared with trastuzumab-conditioned cells. No significant change in the sensitivity to trastuzumab was observed in parental cells during the drug-exposure period (data not shown).

results

inhibitory effect of trastuzumab on growth in breast cancer cell lines

We first screened 17 breast cancer cell lines for *in vitro* growth inhibition using trastuzumab. We confirmed that all relatively sensitive cell lines were *HER2*-amplified (Figure 2A). Among eight *HER2*-amplified cell lines, those with hotspot mutations in *PIK3CA* appeared resistant compared with the remaining cell lines (Figure 2B and C). We categorized BT474 as a *PIK3CA*-wild-type cell line in this study, based on reports showing that the K111N mutation lack ability of transformation and its influence on downstream signaling is negligible [18, 26]. A significant difference in sensitivity at 10 μg/ml trastuzumab was observed between *PIK3CA*-wild-type and -mutant cells (Figure 2C; $P = 0.010$). Protein expression levels of p110-α, the product of *PIK3CA*, were not correlated with sensitivity to trastuzumab (Figure 2C).

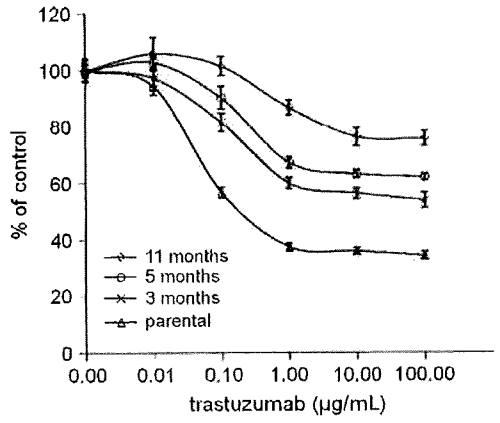

Figure 1. Development of BT474-TR. BT474 cells were continuously exposed to 100 μg/ml trastuzumab. BT-474 and trastuzumab-conditioned BT474 cells were grown in 10% serum-containing media for 5 days in the presence of various concentrations of trastuzumab. The percentage of viable cells is shown relative to that of the untreated control and plotted on the *y*-axis, whereas trastuzumab concentrations are plotted on the *x*-axis. Each data point represents the mean value and standard deviation of 6–12 replicate wells. Trastuzumab resistance increased in cells in a time-dependent manner. After 11 months, cells were designated as BT474-TR.

association between *PIK3CA* mutations and HER2-TKI resistance

Lapatinib, a HER2-TKI which may potentially overcome trastuzumab resistance, has been used in clinical settings [21]. We therefore tested a commercially available HER2-TKI, CL-387,785 [25], on *HER2*-amplified breast cancer cells. As shown in Figure 2D, cell lines with hotspot *PIK3CA* mutations showed resistance to CL-387,785. A statistically significant difference in sensitivity to 1 μM CL-387,785 was observed between *PIK3CA*-wild-type and -mutant cells (Figure 2C; $P = 0.001$) [24].

We then established a trastuzumab-resistant BT474 cell line (BT474-TR), a model of secondary resistant cells, by continuous exposure to trastuzumab (see 'Materials and methods' section). In contrast to *PIK3CA*-mutant cells, which showed primary resistance to trastuzumab, BT474-TR cells remained sensitive to CL-387,785 (Figure 3), which indicates that secondary resistant cells maintain dependency on HER2 signaling for growth.

association between phosphorylation change in S6K and growth inhibition by HER2-targeted agents

To identify potential pharmacodynamic markers of sensitivity to HER2-targeted therapy, we examined changes in phosphorylation of HER2 and representative downstream signaling molecules in 10% FBS-containing media with or without 10 μg/ml trastuzumab or 1 μM CL-387,785 (Figure 4A). The trastuzumab concentration was selected based on maintained growth inhibition (Figure 2B) and wide use in previous studies [11, 19]. The 1-μM CL-387,785 concentration was selected based on the approximate maximum plasma concentration of most TKIs available in clinics to date, including lapatinib [27], and use in previous studies [28, 29].

Trastuzumab treatment resulted in moderate phosphorylation inhibition of Akt and/or S6K in cell lines with wild-type *PIK3CA*. In contrast, no significant changes in Akt and S6K phosphorylation were observed in cell lines with hotspot mutant *PIK3CA*, as well as in BT474-TR cells. Although in ZR75-30, trastuzumab treatment appeared to inhibit phospho-ERK1/2, no significant changes were observed in other sensitive cells, namely BT474 and SKBR-3 (Figure 4A). In addition, phospho-ERK1/2 levels increased in MDA-MB-361 and UACC893, which indicates the presence of compensational cell signaling. Further, with the exception of HCC1419, treatment with CL-387,785 resulted in significant inhibition of Akt and S6K phosphorylation in BT474-TR and *PIK3CA*-wild-type cells, whereas residual phosphorylation signals were observed in all *PIK3CA* hotspot mutant cells.

doi:10.1093/annonc/mdp304 | 257

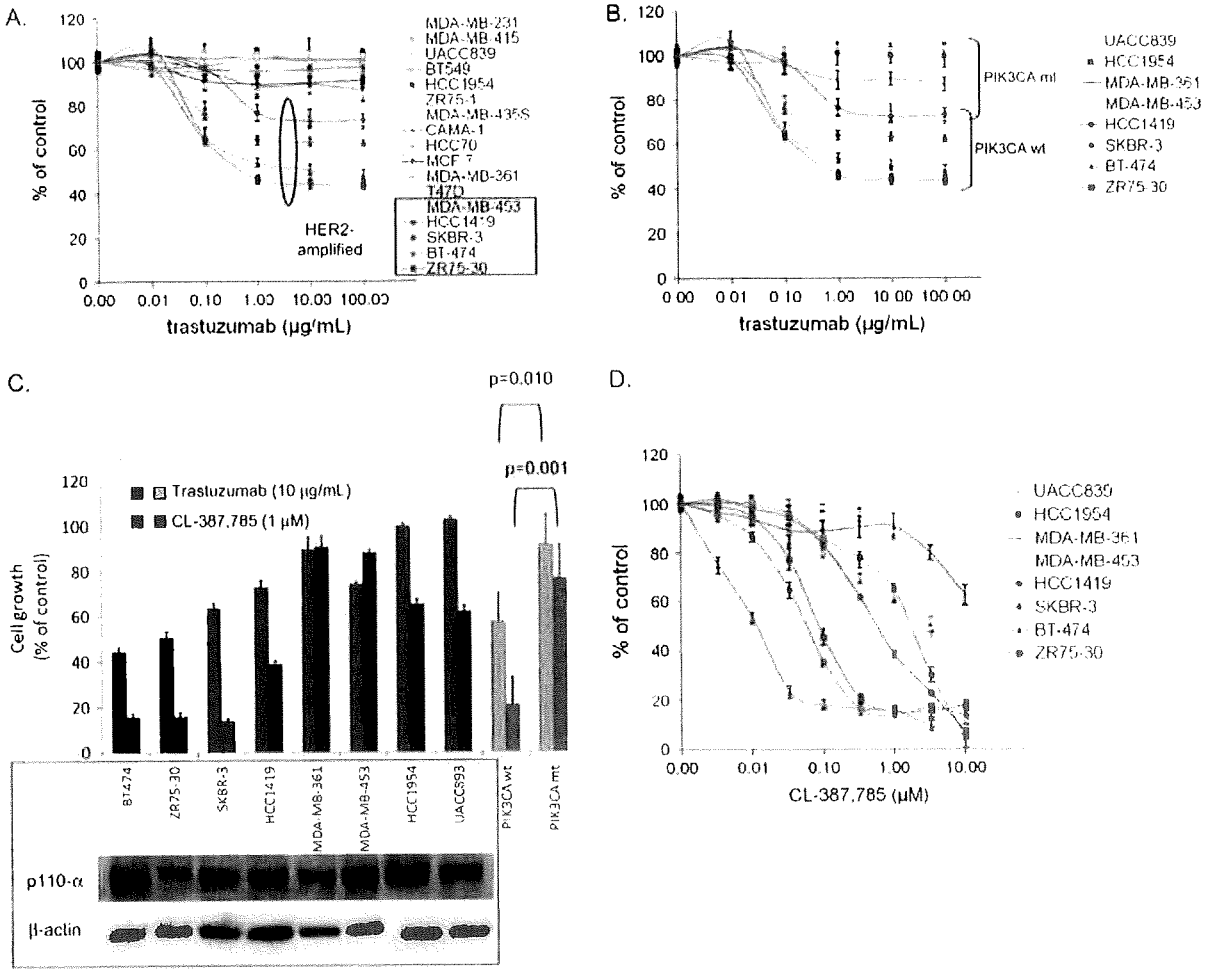

Figure 2. Effect of trastuzumab and CL-387,785 on growth inhibition in breast cancer cells *in vitro* [(A) trastuzumab on 17 breast cancer cell lines; (B) and (D) trastuzumab and CL-387,785 on eight *HER2*-amplified cell lines, respectively]. Breast cancer cells were grown in 10% serum-containing media for 5 days in the presence of various concentrations of trastuzumab (A and B) or CL-387,785 (D). The percentage of viable cells is shown relative to that of the untreated control and plotted on the *y*-axis, whereas trastuzumab and CL-387,785 concentrations are plotted on the *x*-axis. Each data point represents the mean value and standard deviation of 6–12 replicate wells. (C, top) Mean percentage of control and standard deviation of 6–12 replicate wells treated with 10 μg/ml trastuzumab and 1 μM CL-387,785, as well as those of *PIK3CA*-wild-type and -mutant cell lines (bottom), were plotted. (C, bottom) Protein expression of p110-α in *HER2*-amplified breast cancer cells. Blots were stripped and re-probed for β-actin as loading control.

Phosphorylation signals were then quantified and correlated with growth inhibition caused by trastuzumab and CL-387,785. As shown in Figure 4B, the closest association was observed between phospho-S6K changes and growth inhibition caused by trastuzumab and CL-387,785 [correlation coefficient (r), 0.811]. Further, close associations between phospho-S6K and cell growth were consistent when analyzed for trastuzumab and CL-387,785 separately (r for phospho-S6K versus growth: 0.8487 and 0.6970 for trastuzumab and CL-387,785, respectively).

dependency of *HER2*-amplified breast cancer cells on PI3K pathway

Given that inhibition of the PI3K pathway is critical in distinguishing cells sensitive from resistant to HER2-targeted agents (Figure 4B), we evaluated cell lines for the effects of LY294002, a PI3K inhibitor. As shown in Figure 5A, with the exception of ZR75-30, LY294002 induced a >30% growth inhibition compared with control in all cell lines. No significant difference in LY294002 sensitivity was observed between *PIK3CA*-mutant and -wild-type cell lines (Figure 5; $P = 0.655$). These results indicate that most *HER2*-amplified cells at least partly depend on the PI3K pathway regardless of the presence or absence of *PIK3CA* hotspot mutations.

To further gain insight into this concept, we evaluated phosphorylation levels of Akt and ERK1/2 in protein extracts obtained from cells under serum-starved conditions for 24 h. As shown in Figure 5B, despite the absence of serum factors, all *HER2*-amplified breast cancer cells showed a high level of phospho-Akt, regardless of *PIK3CA* genotype. High levels of phospho-Akt were also observed in MDA-MB-468, which lacks PTEN [30], and T47D, which harbors a *PIK3CA* mutation

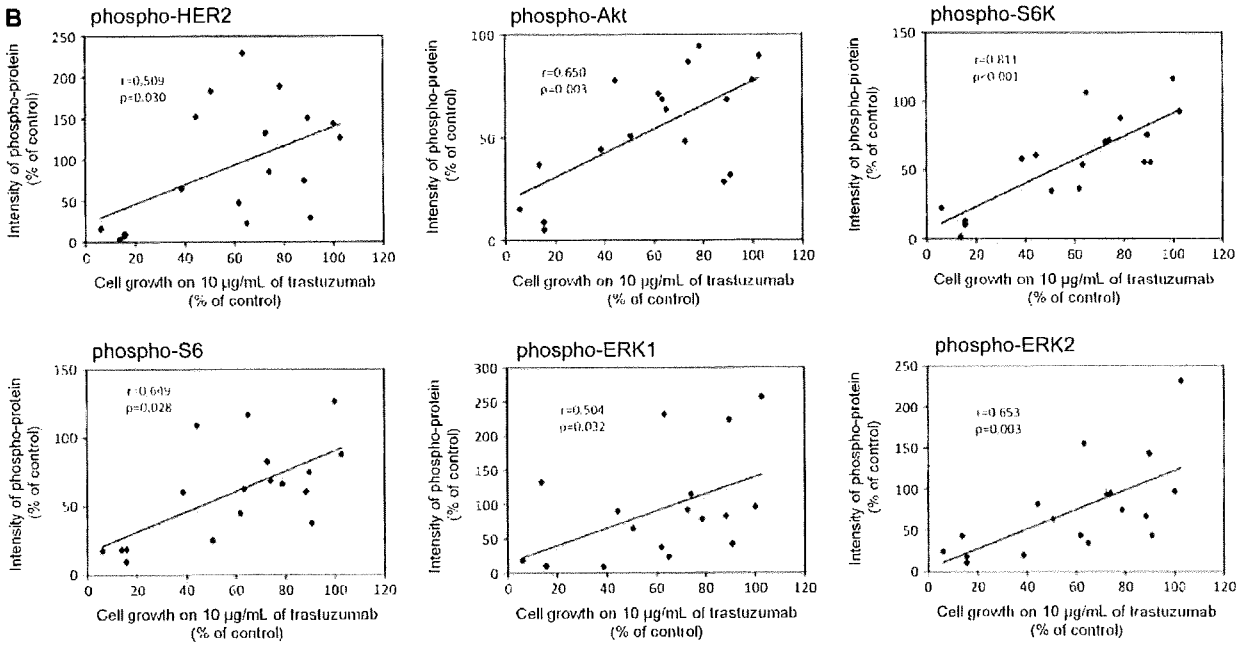

Figure 4. (Continued) (B) Correlation between changes in phosphorylation of HER2 signaling molecules and cell growth. Immunoblot quantification was carried out by densitometry using ImageJ software. Correlations were analyzed by calculating Pearson's correlation coefficient.

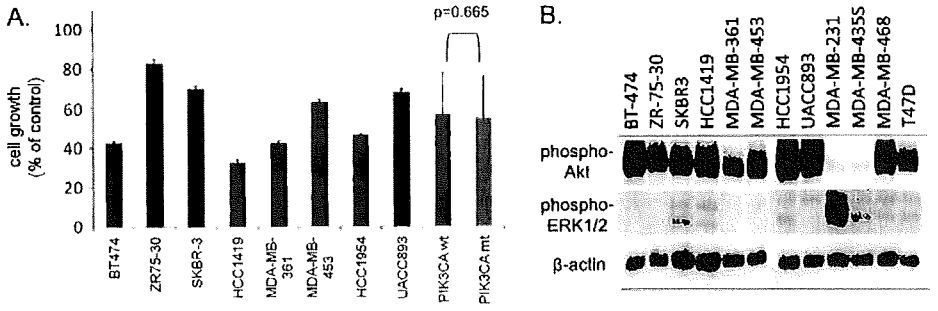

Figure 5. (A) Effect of LY294002 on growth inhibition in HER2-amplified breast cancer cell lines. Mean percentage of control and standard deviation of 6–12 replicate wells treated with 10 μM LY294002 were plotted. (B) Protein expression of phospho-Akt and phospho-ERK1/2 in HER2-amplified breast cancer cells under serum-starved condition. Blots were stripped and re-probed for β-actin as loading control.

(Figure 2C). A study by Haverty et al. [32], which analyzed copy number alterations in 51 breast tumors using a high-resolution single nucleotide polymorphism array, showed no gain in copy number on chromosome 3p, the location of the *PIK3CA* gene. These results indicate that qualitative changes in the *PIK3CA* gene itself may cause trastuzumab resistance in naturally derived breast cancer cells.

The CL-387,785 HER2-TKI was first evaluated to identify groups of compounds which may overcome trastuzumab resistance. Of note, results show an association between *PIK3CA* hotspot mutations and CL-387,785 resistance. Further, the difference in sensitivity between *PIK3CA*-wild-type and -mutant cell lines was more significant for CL-387,785 than for trastuzumab (Figure 2C). These results are consistent with a recent study by Eichhorn et al. [22], which showed that transfection of mutant *PIK3CA* (H1047R) in BT474 cells, which are sensitive to lapatinib, results in drug resistance. In contrast, the results of the present study show that BT474-TR cells remain highly sensitive to CL-387,785, which is consistent with a previous study by Konecny et al. [20] which reported that lapatinib remains active against cell lines selected by long-term exposure to trastuzumab. Although the study did not show the effect of lapatinib on cell signaling in secondary resistant cells, our present findings indicate that BT474-TR remains dependent on HER2/PI3K signaling and sensitive to HER2-TKI (Figure 4A).

We then evaluated LY294002 as a model PI3K inhibitor. Results show that *HER2*-amplified cells are generally sensitive to LY294002 regardless of *PIK3CA* genotype (Figure 5A), which indicates that *HER2* amplification is associated with dependency on PI3K pathway. Supporting this notion, all *HER2*-amplified breast cancer cells have high level of phosphorylation of Akt even in serum-starved condition. The Akt phosphorylation levels observed in *HER2*-amplified cells